Nose-to-brain delivery of DHA-loaded nanoemulsions: A promising approach against Alzheimer's disease

Léa Otaegui, Théo Urgin, Taghrid Zaiter, Charleine Zussy, Mathieu Vitalis, Yann Pellequer, Niyazi Acar, Claire Vigor, Jean-Marie Galano, Thierry Durand, et al.

International Journal of Pharmaceutics 670 (2025) 125125

Contents lists available at ScienceDirect

International Journal of Pharmaceutics

journal homepage: www.elsevier.com/locate/ijpharm

Nose-to-brain delivery of DHA-loaded nanoemulsions: A promising approach against Alzheimer's disease

Léa Otaegui [a], Théo Urgin [a,d], Taghrid Zaiter [b], Charleine Zussy [a], Mathieu Vitalis [a], Yann Pellequer [b,d], Niyazi Acar [c,d], Claire Vigor [e], Jean-Marie Galano [e], Thierry Durand [e], Laurent Givalois [a,f], Arnaud Béduneau [b,d], Catherine Desrumaux [a,d,*]

[a] MMDN, University of Montpellier, EPHE, INSERM, Montpellier, France
[b] Université de Franche-Comté, EFS, INSERM, UMR 1098 RIGHT, F-25000 Besançon, France
[c] Eye and Nutrition Research Group, Centre des Sciences du Goût et de l'Alimentation, AgroSup Dijon, CNRS, INRAE, Institut Agro, Université de Bourgogne Franche-Comté, F-21000 Dijon, France
[d] LipSTIC LabEx (ANR-11-LABX0021), Dijon, France
[e] IBMM, Pôle Chimie Balard Recherche, Université de Montpellier, CNRS, ENSCM, 34293 Montpellier, France
[f] Laval University, Faculty of Medicine, Department of Psychiatry and Neurosciences, CR-CHUQ, Québec City (QC), Canada

ARTICLE INFO

Keywords:
Alzheimer's disease
Omega-3 polyunsaturated fatty acids
Docosahexaenoic acid
Intranasal administration
Nanovectorization
Nanoemulsion
Oxidative stress
Neuroinflammation
Amyloid plaques

ABSTRACT

Reduced docosahexaenoic acid (DHA) concentrations seem to be associated with an increased risk of Alzheimer's disease (AD), and DHA accretion to the brain across the blood–brain-barrier (BBB) can be modulated by various factors. Therefore, there is an urgent need to identify an efficient and non-invasive method to ensure brain DHA enrichment. In the present study, a safe and stable DHA-enriched nanoemulsion, designed to protect DHA against oxidation, was designed and administered intranasally in a transgenic mouse model of AD, the J20 mice.

Intranasal treatment with nanoformulated DHA significantly improved well-being and working spatial memory in six-months-old J20 mice. These behavioral effects were associated with a reduction of amyloid deposition, oxidative stress, and neuroinflammation in brain tissues, which may be partially due to DHA-induced inactivation of the pleiotropic kinase GSK3β.

In conclusion, intranasal DHA administration exhibited strong therapeutic effects and disease-modifying benefits in the J20 AD model. Given that DHA has already shown safety and tolerability in healthy human subjects, our results further support the need for clinical trials to assess the potential of this approach in Alzheimer's patients.

1. Introduction

Alzheimer's disease (AD) is a multifaceted neurodegenerative disorder that accounts for 80 % of dementia cases worldwide, with a prevalence correlated with the aging of the population. The etiology of AD is complex, and sporadic forms, which represent over 95 % of all cases, are thought to arise from interactions between aging, environmental factors and genetic determinants (Arvanitakis, 2024; Rahman et al., 2020). In particular, a number of genes involved in lipid metabolism and transport can modulate the risk of developing AD. The lack of effective treatments makes AD a major public health issue, as patients become entirely dependent due to memory loss, disorientation and motor dysfunction. In addition to amyloid-β (Aβ) plaques and intraneuronal neurofibrillary tangles which are the two histological hallmarks of the AD brain, multiple pathological processes contribute to disease progression including oxidative stress, neuroinflammation, synaptic loss, and brain atrophy (Rathee et al., 2024).

Polyunsaturated fatty acids (PUFAs) from the omega-3 series are a class of fatty acids known for their strong antioxidant and anti-inflammatory properties (Dighriri et al., 2022). The most abundant PUFA in the brain, docosahexaenoic acid (DHA, C22:6n-3), plays a crucial role in brain development and in maintaining proper cognitive functions in adults (Mallick et al., 2019). Several studies have reported reduced brain DHA levels in AD patients (Prasad et al., 1998), and low plasma DHA concentrations have been linked to impaired memory, reduced hippocampal volumes, and increased amyloid deposition (von

* Corresponding author.
E-mail address: catherine.desrumaux-piazza@umontpellier.fr (C. Desrumaux).

https://doi.org/10.1016/j.ijpharm.2024.125125
Received 16 October 2024; Received in revised form 2 December 2024; Accepted 21 December 2024
Available online 7 January 2025

Schacky, 2021).

DHA synthesis through the bioconversion of the essential α-linolenic acid (ALA, C18:3n-3) in the liver is marginal in humans, making it necessary to obtain DHA from external sources such as diet or supplements (Plourde and Cunnane, 2007). Modern diets contain low amounts of DHA, and supplementation is regarded as a promising strategy for the primary prevention of AD (Gao et al., 2011; Mohajeri et al., 2015; Zhang et al., 2015).

Several studies have shown that long-term DHA supplementation has anti-amyloidogenic properties in AD animal models, diminishing neuronal loss and improving cognitive functions (Cole and Frautschy, 2006; Hooijmans et al., 2009; Oster and Pillot, 2010; Teng et al., 2015; Lim et al., 2005). In humans, while numerous epidemiological studies suggest that dietary DHA consumption may protect the elderly from developing cognitive impairment or dementia including AD, review articles report an inconclusive association between omega-3 PUFA intake and cognitive decline (Gillette Guyonnet et al., 2007; Maclean et al., 2005; Plourde et al., 2007). One possible explanation is that DHA accretion across the Blood Brain Barrier (BBB) can be modulated by a variety of factors such as age, nutrition, and genetic polymorphisms (Lo Van et al., 2016; Pan et al., 2015). In addition, due to DHA structure, with six double bonds and five methylene carbons, it is more susceptible to oxidation than linoleic, linolenic, and arachidonic acids (Witting and Horwitt, 1964). Controlling DHA oxidation is crucial to avoid discrepancies in preclinical and clinical studies. Currently, there is a urgent need for new strategies to overcome these two limitations and optimize brain DHA delivery to the brain.

Direct intranasal administration has recently emerged as a promising alternative to the oral and parenteral routes to target the central nervous system (CNS). This route of administration bypasses the BBB and enables molecules to reach the CNS via the olfactory and trigeminal nerves. The main advantages of the intranasal route include (i) its accessibility, (ii) its non-invasiveness, and (iii) its very low metabolic activity (compared to the gastrointestinal tract), resulting in high bioavailability (Erdő et al., 2018; Kumar et al., 2018). This strategy has recently been validated in clinical trials for cerebral insulin delivery (Hallschmid, 2021) and is currently being evaluated for other drugs such as acetylcholinesterase inhibitors (Zhao et al., 2021). This study builds on prior work from our group, showing that intranasal administration of DHA is a viable alternative to traditional oral supplementation (Zussy et al., 2022). It introduces an improved DHA formulation, likely with enhanced stability and protection against oxidation, addressing a key challenge in DHA supplementation which could significantly improve the outcomes in clinical and preclinical studies. The research focuses on assessing its potential to reduce amyloid deposition and neuroinflammation in the hippocampus, as well as improving cognitive functions in a transgenic Alzheimer's disease (AD) mouse model. In summary, the study's novel approach using intranasal DHA aims to overcome the challenges of DHA delivery and oxidation, offering a promising strategy to counteract DHA depletion in the aging brain and prevent neurodegeneration.

2. Materials and methods

2.1. DHA-loaded nanoemulsions: Preparation and characterization

2.1.1. Preparation

The nanoemulsions (NEs) were prepared and characterized by Dr. Béduneau's team, following a previously published process (Jamoussi et al., 2021). Their composition consisted of 13.1 % (w/w) Kolliphor® HS15, 3.7 % (w/w) oil, and 83.2 % (w/w) deionized water. The oil phase of DHA-NEs comprised 80—100 % (w/w) Omegavie® DHA-rich oil (Polaris, Quimper, France) and 0–20 % (w/w) Labrafac® Lipophile WL 1349 (Gattefossé, Saint-Priest, France). The incorporation of Labrafac® was required in some batches of the natural product Omegavie® DHA-rich oil to achieve the desired particle size of approximately 30 nm. Conversely, the oil phase in the vehicle-NEs consisted entirely of Labrafac®. The same formulation process was used for both DHA-NEs and vehicle-NEs. In brief, the oil phase containing Kolliphor® HS15, and deionized water were separately heated to 90 °C in a water bath and degassed under nitrogen. The water phase was then injected into the lipid phase using a syringe. After mixing at 90 °C under a nitrogen atmosphere, the formulation was cooled to room temperature under magnetic stirring. The NEs were subsequently filtered through a 0.20 μm cellulose acetate membrane under sterile conditions and transferred into 2-mL amber vials. Finally, the NEs were degassed under nitrogen and stored at 4 °C.

2.1.2. Particle size and polydispersity measurements

The size and the polydispersity index (PDI) of NEs were measured at 25 °C using a Zetasizer Nano ZS 90, (Malvern Instruments, Orsay, France). All measurements were performed in triplicate after a 1:10 dilution in deionized water.

2.1.3. DHA content

The DHA concentration in NEs was determined according to previously described procedures (Acar et al., 2021, 2012). Lipids were extracted according to the Folch method (Folch et al., 1957). Total lipids were extracted with 5 ml of a chloroform/methanol mixture (2:1, v/v), then the samples were centrifuged at 1860 × g for 3 min and the lower organic phase was isolated and evaporated to dryness under a stream of nitrogen. Finally, total lipids were dissolved in hexane and stored under nitrogen at − 20 °C until further analyses. The fatty acids were transmethylated using boron trifluoride in methanol according to Morrison and Smith (Morrison and Smith, 1964). The fatty acid methyl esters formed by transmethylation were extracted with hexane. They were analyzed on a Trace 1310 gas chromatograph (Thermo-Scientific, Courtaboeuf, France) equipped with a CPSIL-88 column (100 m × 0.25 mm i.d., film thickness 0.20 μm; Varian, Les Ulis, France) and a flame ionization detector. Hydrogen was used as a carrier gas (inlet pressure 210 kPa). The oven temperature was held at 60 °C for 5 min, increased to 165 °C at 15 °C/min and held for 1 min, then increased to 225 °C (2 °C/min), and finally held at 225 °C for 7 min. The injector and the flame ionization detector were maintained at 250 °C. DHA methyl esters were identified by comparison with commercial and synthetic standards. The data were computed using the Chromeleon software (version 7.1.10 ES, Thermo Scientific, Courtaboeuf, France).

2.1.4. Toxicity assessment

Since we use intranasal administration, the toxicity of the nanoformulations was evaluated in the RPMI 2650 nasal epithelium cell line. RPMI 2650 cells (passages 5 to 20) were cultured in Eagle's minimal essential medium (EMEM) supplemented with 10 % FBS and 1 % penicillin/streptomycin. They were plated in 96-well plates at a density comprised between 100,000 and 200,000 cells/well and allowed to adhere at least overnight in the incubator with 5 % CO_2 at 37 °C before the experiment. Cells were then rinsed with DPBS and treated with various concentrations of vehicle-NEs for 2 h in culture medium. At the end of the incubation period, cell viability was determined using the MTS (3-(4,5-dimethylthiazol-2-yl)-5-(3-carboxymethoxyphenyl)-2-(4-sulfophenyl)–2H-tetrazolium, Sigma-Aldrich) test. Based on the Promega protocol, 20 μl MTS reagent were added in each well containing 100 μl culture medium for 1–2 h at 37 °C and 5 % CO_2. A microplate reader (Multiskan Sky, Thermoscientific) was used to measure the absorbance at 490 nm.

2.1.5. Antioxidant capacity

The oxygen radical absorbance capacity (ORAC) assay was performed to assess the antioxidant capacity of NEs, using Trolox as a positive control (Huang et al., 2002). Briefly, 25 μl of NEs or Trolox were pipetted in a 96-well white microplate (with clear bottom), whereas phosphate buffer (25 μl, 75 mM, pH 7.4) was transferred in the negative

control wells. Fluorescein solution (150 µl, 25 nM) was added in each well and the plate was incubated in the dark at 37 °C for 30 min. Subsequently, 2,2′-azobis (2-amidinopropane) dihydrochloride (AAPH) solution (25 µl, 0.15 M) was added in the positive control and the antioxidant wells, whereas phosphate buffer (25 µl) was pipetted in the negative control, and the fluorescence was measured every 2 min over a period of 2 h (485/20 nm excitation, 525/20 nm emission) using a Fluoroskan Ascent microplate reader (ThermoScientific, Waltham, MA, USA).

2.2. In vivo Evaluation of nanoemulsions

2.2.1. Animals and treatment protocol

Hemizygous $hAPP_{SwInd}$ transgenic (J20) mice were purchased from the Jackson Laboratories. A Material Transfer Agreement (#UM140255-01) was signed with the Gladstone Institute for their use. J20 mice were on the C57BL/6J background and backcrossed more than 10 generations. Wild-type (WT) littermate mice were used as controls. The genotyping of the J20 mice has been described previously (Mansuy et al., 2018). Six-months-old male and female animals were used throughout this study. Mice were treated 2 weeks, 5 times/week, by intranasal administration of either DHA-NEs (DHA dose, 10 mg/kg) or vehicle-NEs, and behavioral phenotyping was performed at the end of the treatment period. Deeply anesthesized animals were then sacrificed by cardiac perfusion.

All mice were housed in a standard animal facility (12L/12D cycle, 21 ± 2°C) with free access to water and food (A03 diet, SAFE Diets, France). All procedures were conducted in strict adherence to the European Union Directive of September 22, 2010 (2010/63/UE). This project followed the specific French national guidelines on animal experimentation and well-being. The national French animal welfare committee and the local committee at the University of Montpellier approved all protocols (*authorization: CEEA-LR-6914*). All efforts were made to minimize the number of animals used, potential pain, suffering and distress.

2.2.2. Behavioral tests

A series of behavioral tests was performed to evaluate and compare the cognitive performances of WT, vehicle-NEs-treated J20 mice and DHA-NEs-treated J20 mice. Behavioral experiments were all performed between 08:00 AM and 01:00 PM.

2.2.2.1. Nesting test. To evaluate their organizational skills and well-being, mice were placed individually in polysulfone cages with bedding about 1 h before the dark phase. Cotton nestlets (Plexx®, The Netherlands) were provided as nesting material (1/cage), and nesting behavior was assessed the next morning. The nests were scored by two independent observers blind to the group identity, according to the following scale: 0 = undisturbed; 1 = disturbed; 2 = flat nest; 3 = cup-shaped nest; 4 = incomplete dome; 5 = complete dome (Hess et al., 2008). Mean nesting scores were compared between groups.

2.2.2.2. Spatial working memory assessment (Y-Maze Test). Spontaneous alternation behavior, which is a measure of spatial working memory, is driven by an innate curiosity of rodents to explore previously unvisited areas and was tested using a Y-maze following a previously described protocol (Desrumaux et al., 2013; Mansuy et al., 2018). Each animal was placed in the center of the maze and allowed to freely explore the three arms during 8 min. The number of arm entries and the number of triads (alternations) was evaluated to calculate the percentage of alternations ((actual alternations/maximum alternations) × 100) using the EthoVisonXT14 (Noldus, Wageningen, The Netherlands) video-tracking system.

The apparatus was cleaned with diluted ethanol (50 %) between each session.

2.2.2.3. Splash test. This test was performed to evaluate the depressive-like behavior of the mice. Briefly, the dorsal coat of mice was squirted with a 10 % sucrose solution (w/v). Due to its viscosity, the sucrose solution dirties the coat and initiates a grooming behavior. The latency to the first grooming and the total grooming duration (over a 5-min period) were recorded by a blinded observer, as indexes of self-care and motivational behavior (Kong et al., 2023; Moretti et al., 2012; Willner, 2005).

2.2.3. Tissue preparation for histological and biochemical analyses

Mice were anesthetized with a ketamine (100 mg/kg)/xylazine (10 mg/kg) mixture and euthanized by cardiac perfusion with PBS. The brains were carefully removed and sagittally divided; the left hemisphere was snap frozen and stored at −80 °C; on the right hemisphere, the prefrontal cortex was harvested, snap frozen and stored at −80 °C; then the rest of the right hemisphere was post-fixed in 4 % paraformaldehyde (AntigenFix®, Diapath France) for 48 h at 4 °C, and transferred into a 30 % sucrose solution for 3 days. Tissues were then included in a block of OCT compound (Tissue-Tek®, Sakura Finetek, USA) and quickly frozen in acetone chilled on dry ice. Frozen blocks were mounted on a cryostat (Leica, France) and 25 µm-thick coronal sections were collected and stored at −20 °C in anti-freeze solution. Frozen, left hemi-brains were homogenized using an ultrasound probe in phosphate buffer containing protease and phosphatase inhibitors (Complete Ultra, Roche, Switzerland − Phostop, Sigma-Aldrich). Homogenates were centrifuged at 20,000 x g for 30 min at 4 °C and the supernatants protein concentrations were measured using the bicinchoninic acid method (Pierce BCA kit/ Thermofisher Scientific, France). They were then stored in aliquots at −80 °C until use for Western Blot analyses.

2.2.4. Oxidative stress markers quantification

Non-enzymatic oxygenated polyunsaturated fatty acid metabolites (NEO-PUFAs) were extracted from prefrontal cortex tissue, and the qualitative and quantitative profile of these lipid mediators was determined by micro-LC-MS/MS as previously described (Roy et al., 2020). Their concentration was established by calibration curves calculated from the area ratio of analytes and the internal standards. Data processing was performed using a MultiQuant 3.0 software (Sciex Applied Biosystems, Framingham, USA).

2.2.5. Immunohistochemical analysis of neuro-inflammatory markers

Analysis of the astrocytic activation marker GFAP and of the microglial marker Iba-1 was conducted by fluorescence immunohistochemistry. Free-floating coronal sections (taken from the anterior hippocampus level with intervals of 100 µm) were rinsed with PBS to remove cryoprotectants, mounted on Superfrost® Plus glass slides, and dried overnight at room temperature. They were then blocked 1 h at room temperature with 3 % goat serum and incubated overnight at 4 °C with a mouse anti-GFAP antibody (1:1000, Sigma-Aldrich, France) and a rabbit anti-Iba-1 antibody (1:500; Wako Chemicals, Japan). Sections were then incubated for 2 h with goat anti-mouse fluorescent (Cy3) (Jackson Immunoresearch, USA) and goat anti-rabbit fluorescent (AlexaFluor 488) (Thermo Fisher Scientific, France) secondary antibodies. Nuclei were counterstained with 4′,6′-diamino-2-phenylindole (DAPI) (Molecular Probes/Thermo Fisher Scientific, France). The immunostaining specificity was determined with the same protocol but by incubating control sections with the secondary antibody alone.

The Iba-1 and GFAP slides were captured using the 20x magnification lens of the Leica THUNDER Imager Tissue Microscope. Four to six sections per animal were used for the cell counting. Three fields per section (1 in dentate gyrus, 1 in CA1, 1 in CA3) were used to manually count GFAP-positive and Iba-1 positive cells. All measurements were performed by an investigator that was blinded to the identity of the mouse brains.

2.2.6. Quantification of amyloid plaques in hemibrain tissue sections

Amyloid deposits were stained using the fluorescent dye Thioflavin T (ThT) (Sigma-Aldrich). Briefly, free-floating coronal sections (taken from the anterior hippocampus level with intervals of 100 μm) were rinsed with PBS to remove cryoprotectants, mounted on Superfrost® Plus glass slides, dried overnight at room temperature, incubated with a ThT solution at 0.01 % (31 μM) for 10 min, dehydrated with 70 % and 80 % ethanol solutions and counterstained with DAPI (1:50,000) (Molecular Probes). All sections were visualized under a Leica DM2500 microscope (Leica Microsystems) (magnifications: ×20 and × 40 for enlargements). Images were analyzed with Fiji software (version 2.0; National Institutes of Health). Hemi-brain tissue sections were used to quantify the number and the surface area of amyloid plaques in the hippocampus. Eight to 10 sections were used per animal, and all the values obtained were pooled to get the total number and total surface area of aggregates. These data were then normalized to the surface area of the half-hippocampus of the quantified section.

2.2.7. Western blotting

After adjustment to the same protein concentration (3 μg/μl), hemi-brain homogenates were diluted (1:1) in Laemmli buffer, boiled for 5 min, loaded and separated on a 12 % polyacrylamide gel (sixty micrograms protein/lane), then transferred to a polyvinylidene difluoride membrane (Whatman, Versailles, France). After protein transfer, the membrane was blocked in 5 % non-fat dry milk, incubated overnight (4 °C) with the primary antibody, rinsed, and incubated for 2 h with the appropriate horseradish peroxidase-conjugated secondary antibody (Sigma-Aldrich, Saint Quentin Fallavier, France). Peroxidase activity was revealed using enhanced chemiluminescence (ECL) reagents (Luminata Crescendo, Millipore, Molsheim, France). The intensity of peroxidase activity was quantified using Image Lab Software 6.1 (Bio-Rad, Hercules, USA). Total GSK3β was used as loading control.

Primary antibodies used were the following: mouse anti-GSK3β (1:2000, #610202, BD Biosciences, France), mouse anti-GSK3β pTyr216 (1:2000, #612313, BD Biosciences, France), rabbit anti-GSK3β pSer9 (1:1000, #9336, Cell Signalling Technology/Ozyme, France).

2.3. Statistical analysis

The data are presented as mean ± SEM. Before each analysis of variance, the Gaussian distribution was systematically evaluated and validated by a Kolmogorov–Smirnov test (GraphPad Prism 9.5.1, San Diego, USA). Data sets were analyzed using parametric (ANOVA) or non-parametric (Mann-Whitney) analysis of variance, followed by a Tukey's or Dunn's multiple comparison test, respectively (GraphPad Prism 9.5.1). A p value of less than 0.05 was considered significant.

3. Results

3.1. Characterization, DHA stability and antioxidant capacity of NEs

The size and polydispersity index (PDI) of freshly prepared DHA-NEs and vehicle-NEs are presented in Table 1. The mean hydrodynamic diameter of the DHA-NEs was 28.8 nm. DHA slightly increased the size of the droplets compared to vehicle-NEs prepared with Labrafac alone, which were characterized by a hydrodynamic diameter of 22 nm. The polydispersity index of DHA-NEs and vehicle-NEs was 0.09 and 0.072, respectively, indicating a monomodal size distribution for both formulations.

Since DHA is highly susceptible to oxidation, we evaluated its stability in NEs. This analysis revealed that the amount of DHA in DHA-NEs was constant upon storage at 4 °C under nitrogen over a 5 months period (Table 2).

We next evaluated the antioxidant potential of DHA-NEs and Vehicle-NEs using the ORAC assay. As shown in Fig. 1, we observed that DHA-NEs, but not vehicle-NEs, display a strong antioxidant potential, that remained stable after 3 months of storage at 4 °C (data not shown).

3.2. Effect of DHA-NEs treatment on cell viability in RPMI 2650 cells

The impact of vehicle-NEs and DHA-NEs on cell viability was assessed in the nasal epithelium cell model RPMI 2650 by using the MTS assay. As shown in Fig. 2, incubation of RPMI 2650 cells with up to 10 % of either vehicle-NEs or DHA-NEs in the culture medium did not induce significant changes in cell viability.

3.3. Effect of intranasal DHA-NEs treatment on cognitive impairment in the J20 murine AD model

We next addressed the impact of intranasal administration of DHA-NEs on cognitive performances in the J20 mouse model. For this purpose, mice were treated intranasally with either a saline solution (WT group), vehicle-NEs (J20 control group), or DHA-NEs (J20 experimental group), 5 days/week for 2 weeks. Then, behavioral tests were conducted in parallel in WT mice, vehicle-NEs treated J20 mice and DHA-NEs treated J20 mice. As shown in Fig. 3A, altered performances in the nesting test were observed in vehicle-NEs treated mice compared to WT mice, indicating reduced well-being and organizational skills (nesting score: 1.2 ± 0.3 *vs* 2.4 ± 0.3 in vehicle-NEs treated J20 mice and WT mice, respectively, $p < 0.05$). In addition, spatial working memory −assessed using the Y-maze test by measuring the mouse ability to spontaneously alternate during maze exploration- was reduced by 20 % in vehicle-NEs treated J20 mice compared to WT mice (alternation %: 47.6 ± 2.8 *vs* 63.7 ± 2.9, $p < 0.01$) (Fig. 3B). The splash test, performed to assess depressive-like behavior, revealed a significant difference in grooming time and latency to the first grooming between vehicle-NEs treated J20 mice and WT mice (grooming time, 40.9 ± 5.3 s *vs* 86.1 ± 5.1 s, $p < 0.001$; latency, 20.2 ± 3.5 s *vs* 6.1 ± 1.9 s, $p < 0.0001$) (Fig. 3C), indicating a strong apathetic behavior in J20 mice. Intranasal administration of DHA-NEs to J20 mice resulted in a significant improvement of their well-being (nesting score: 2.4 ± 0.3, $p < 0.05$ *vs* vehicle-NEs treated J20 mice), and fully restored spatial memory deficits (alternation %: 63.7 ± 3.9, $p < 0.05$ *vs* vehicle-NEs treated J20 mice). Regarding depressive behavior, tendencies were observed. Notably, no differences in total mobility in the Y-maze were measured between J20 mice treated with Vehicle-NEs or DHA-NEs.

3.4. Effect of intranasal DHA-NEs treatment on oxidative stress and neuroinflammation in the J20 murine AD model

As shown in Table 3, biochemical assays performed on prefrontal cortex homogenates revealed that cerebral levels of the oxidative stress markers 5-F_{2c}-Isoprostanes and 10(S)-10-F_{4t}-Neuroprostanes were significantly decreased in DHA-NEs-treated J20 mice, but not vehicle-NEs-treated J20 mice, compared to WT mice.

To determine the impact of DHA-NEs treatment on astrogliosis and

Table 1
Average size and polydispersity index (PDI) of at least 3 batches of DHA-NEs and Vehicle-NEs.

	DHA-NEs	Vehicle-NEs
Size (nm)	28.8 ± 5.3	22.0 ± 0.3
PDI	0.090 ± 0.018	0.072 ± 0.040

Table 2
DHA content of nanoemulsions upon storage.

Months after formulation	**0**	**1**	**2**	**3**	**4**	**5**
DHA content, mg/ml	18.7 ± 0.2	19.1 ± 0.3	18.4 ± 0.7	19.5 ± 0.5	18.9 ± 0.5	17.1 ± 0.6

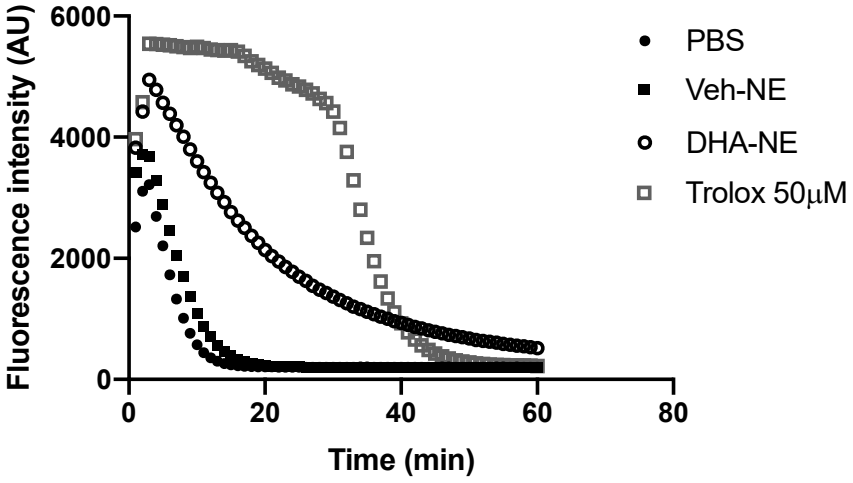

Tested product	Net AUC
Trolox 50 µM	153.5
Veh-NE	7.7
DHA-NE	80.5

Fig. 1. Comparison of the antioxidant potential of vehicle-NEs (Veh-NEs) and DHA-NEs. The ORAC assay was performed and fluorescence decay curves for the negative control (PBS), vehicle-NEs, DHA-NEs and the positive control (Trolox) are presented. In the Table, the net AUCs were calculated by subtracting the blank (PBS) AUC value.

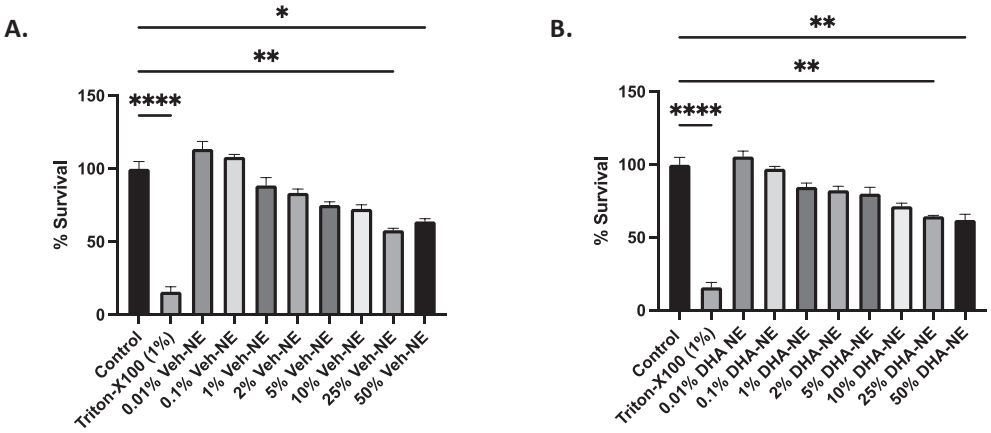

Fig. 2. Impact of Vehicle-NEs and DHA-NEs on cell survival. Nasal epithelium RPMI 2650 cells were seeded in 96-well culture plates at 4×10^4 cells per well and cultured for 24h. The cells were then incubated the absence (Control) or presence of varying concentrations of vehicle-NEs or DHA-NEs for 2h. Triton X-100 (1%) was used as a control for maximal toxicity. Cell viability was assessed by measuring MTS reduction. Values represent the mean ± SEM of 5–8 assays and are expressed as a percentage of the control. * $p < 0.05$; ** $p < 0.01$; **** $p < 0.0001$ *vs* control conditions (Mann-Whitney non-parametric test).

microgliosis, the numbers of GFAP- (Fig. 4) and Iba1- (Fig. 5) positive cells were determined in the hippocampal region of brain sections by immunohistochemistry. As shown in Fig. 4B, a significant increase in the number of GFAP-positive cells was measured only in the dentate gyrus and CA3 areas of brain sections from vehicle-NEs treated J20 mice compared to WT mice. In DHA-NEs treated J20 mice, the number of GFAP-positive cells was significantly reduced in the dentate gyrus area, and not significantly different from that measured in WT mice. In the CA1 area, no differences were observed between groups. Representative pictures of GFAP immunostaining in the different areas and groups are presented in Fig. 4A.

The numbers of microglial cells were quantified in the hippocampus of WT, vehicle-NEs treated J20 mice and DHA-NEs treated J20 mice (Fig. 5). Our immunohistochemical analysis revealed a significant increase in the number of microglial cells (Iba1-positive) in the dentate gyrus and CA3 areas of brain sections from vehicle-NEs treated J20 mice compared to WT mice ($p < 0.01$). In DHA-NEs treated J20 mice, the number of Iba1-positive cells was significantly reduced in both areas ($p < 0.01$), and not different from that measured in WT mice (Fig. 5B). In the CA1 area, no differences were measured between groups. Representative pictures of Iba1 immunostaining in the different areas and groups are presented in Fig. 5A.

3.5. Effect of intranasal DHA-NEs treatment on amyloid deposition in the J20 murine AD model

The impact of DHA-NEs treatment on amyloid deposition was carried out by histological analyses using ThT staining. The number and size of

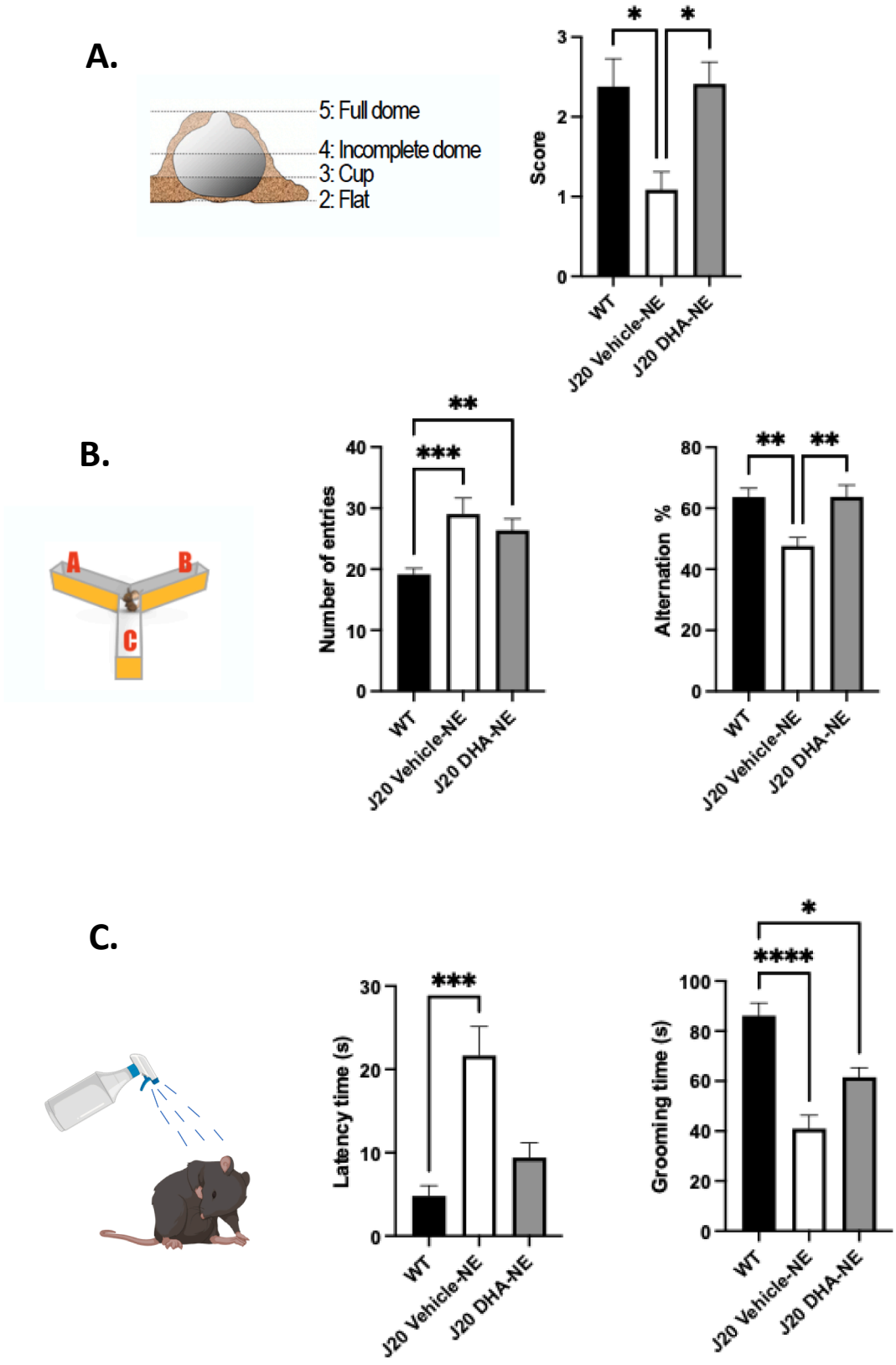

Fig. 3. Behavioral assessment. The nesting (**A**), Y-maze (**B**) and splash (**C**) tests were performed to assess general welfare behavior, working spatial memory, and depressive state, respectively. (**A**) The nesting score (scale 0–5) was established by two independent observers blind to the group identity. (**B**) The number of arm entries (left panel) and the number of alternations were recorded to calculate the percentage of alternations (right panel). (**C**) The latency to the first grooming (left panel) and total grooming time (right panel) are presented. Results are presented as mean ± SEM. Statistical analysis of variance was performed using the Mann-Whitney (A and B) or ANOVA (C) tests, as appropriate. * $p < 0.05$; ** $p < 0.01$; *** $p < 0.001$; **** $p < 0.0001$.

Table 3
Oxidative stress markers assessment in prefrontal cortex homogenates.

	WT	Vehicle-NEs-treated J20	DHA-NEs-treated J20
5-F2c-Isoprostanes (pg/mg)	14.35 ± 2.26	11.95 ± 2.85	9.22 ± 2.00 **
10(S)-10-F4t-Neuroprostanes (pg/mg)	1.55 ± 0.24	1.35 ± 0.33	0.98 ± 0.29 **

** $p < 0.01$ *vs* WT.

aggregates were quantified in the hippocampus since it has been previously reported that amyloid plaques are 5–10 times more abundant in the hippocampus than in the cortex in J20 mice (Lafon et al., 2020; Mansuy et al., 2018). As shown in Fig. 6A, the number of hippocampal ThT-positive plaques was significantly lower in DHA-NEs treated animals compared to vehicle-NEs treated animals (2.9 ± 1.1/cm^2 *vs* 9.5 ± 2.4/cm^2, $p < 0.05$). Although a decrease in the total surface area of amyloid plaques was observed in DHA-NEs treated compared to vehicle-NEs treated animals (x1000 values, hippocampus: 4.0 ± 1.0 % *vs* 4.9 ± 0.7 %), the difference was not significant (Fig. 6B). In Fig. 6 (C-D) are displayed representative pictures of ThT-stained brain sections from vehicle-NEs treated animals and DHA-NEs treated J20 mice.

3.6. Effect of intranasal DHA-NEs treatment on GSK3-β kinase activation in the hippocampus

We further assessed the phosphorylation state of GSK3-β, a multifunctional kinase which activity is strongly related to several pathological features of AD, in the brain tissue of WT mice and J20 mice treated with vehicle-NEs or DHA-NEs. As shown in Fig. 7 (A-B), a significant increase of GSK3-β phosphorylation at the Ser9 residue (i.e., inactive GSK3-β) ($p < 0.01$) and a tendency towards decreased phosphorylation at the Tyr216 residue (i.e., active GSK3-β) were observed in DHA-NEs treated J20 mice compared to vehicle-NEs treated J20 mice, suggesting reduced activity.

4. Discussion

PUFAs are a class of substances with numerous beneficial effects on human health. Among them, DHA, an omega-3 fatty acid, is the most abundant PUFA in the brain and is a key regulator of cognitive functions (Mallick et al., 2019).

Reduced DHA levels are a major AD risk factor, and DHA accretion to the brain across the blood–brain-barrier (BBB) is a tightly regulated process. Therefore, there is a need to develop an efficient and non-invasive method to ensure brain DHA enrichment.

A previous study from our group was designed to explore for the first time a route of administration for DHA that bypasses the gastrointestinal tract and the BBB, namely the intranasal administration route. We demonstrated, using two complementary AD mouse models, that intranasal administration of a DHA microemulsion containing Curcumin as a co-antioxidant can efficiently prevent cognitive decline and block tau hyperphosphorylation by acting on JNK signaling. The non-transgenic model was used to screen and select the most efficient microemulsion, while the transgenic model allowed us to demonstrate that the curcumin/DHA microemulsion can counteract endogenous Aβ-induced toxicity (Zussy et al., 2022).

The present study had two main objectives: first, to evaluate the efficacy of a new type of nanovector for DHA that provides protection against oxidative stress; secondly, to determine the impact of intranasal

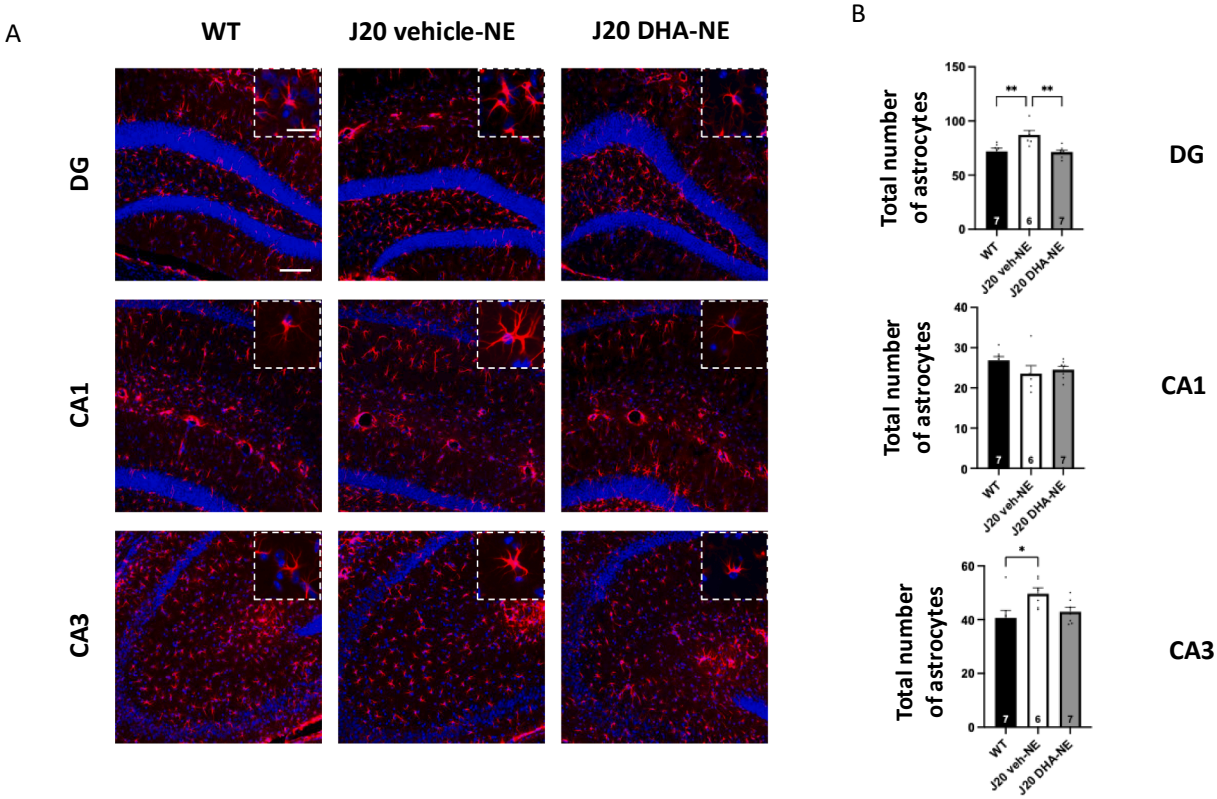

Fig. 4. Quantification of astrocytes in brain sections. (**A**) Representative images of astrocytes labelling (GFAP immunostaining) in the hippocampus region of brain sections of WT (n = 7) and J20 mice, treated with vehicle-NEs (n = 6) or DHA-NEs (n = 7) for 2 weeks. (**B**) The number of astrocyte cells was quantified in the dentate gyrus (DG), CA1, and CA3 areas. Six to eight brain tissue sections per animal were analyzed. Values are expressed as mean ± SEM and statistical analysis was performed using a two-way ANOVA followed by a Tukey's multiple comparisons post hoc test (*$p < 0.05$, **$p < 0.01$). Scale bar: 100 μm (magnification × 20). Inserts show representative images of astrocyte cells status in the different groups (scale bar: 25 μm, magnification × 20).

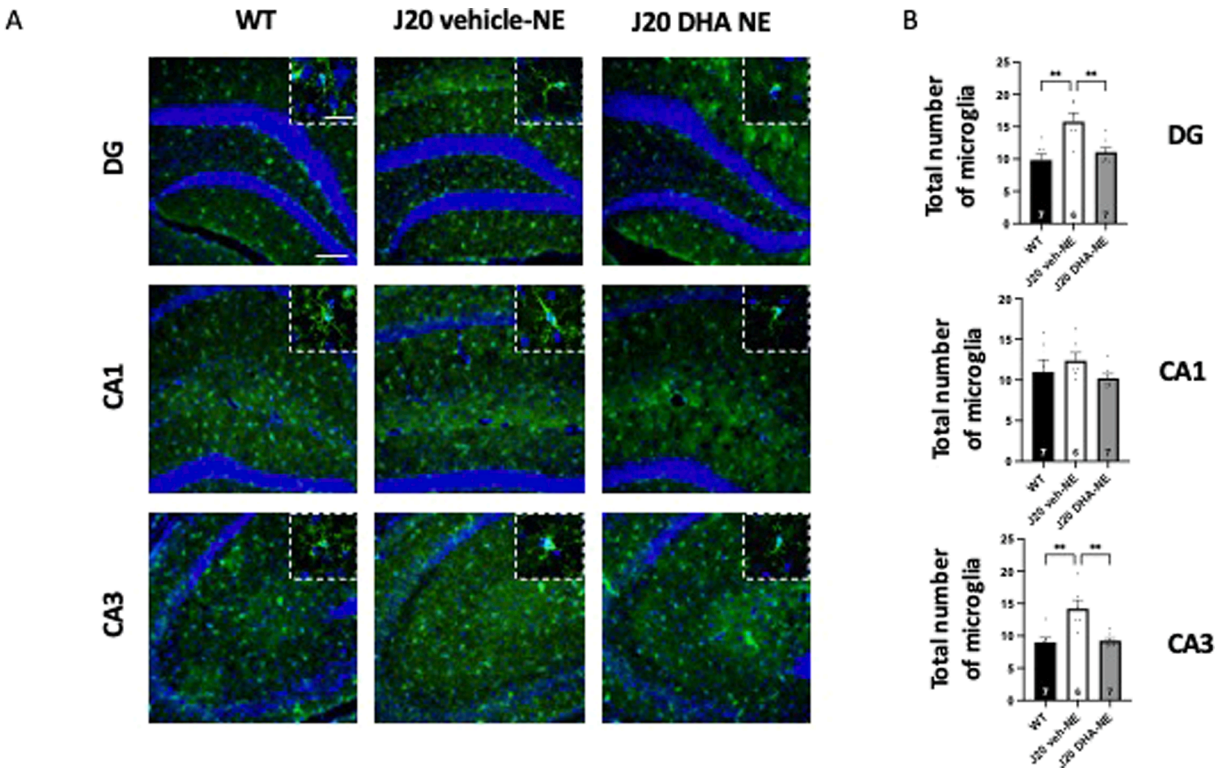

Fig. 5. Quantification of microglia in brain sections. (A) Representative images of microglia labelling (Iba-1 immunostaining) in the hippocampus region of brain sections from WT (n = 7) and J20 mice, treated with vehicle-NEs (n = 6) or DHA-NEs (n = 7) for 2 weeks. (**B**) The number of microglial cells was quantified in the dentate gyrus (DG), CA1, and CA3 areas. Six to eight brain tissue sections per animal were analyzed. Values are expressed as mean ± SEM and statistical analysis was performed using a two-way ANOVA followed by a Tukey's multiple comparisons post hoc test (**$p < 0.01$). Scale bar: 100 μm (magnification × 20). Inserts show representative images of microglial cells status in the different groups (scale bar: 25 μm, magnification × 20).

DHA administration on cognitive functions, oxidative stress, neuroinflammation, amyloid deposition, and the activity of the kinase GSK3β in a transgenic AD model.

4.1. *Stability of DHA in nanoemulsions*

There is currently a strong interest in the utilization of colloidal delivery systems to encapsulate bioactive lipophilic compounds, enabling their solubilization in aqueous media and delivery to target organs (Liu et al., 2024). Among the numerous systems that have been developed −including microemulsions, nanoemulsions, emulsions, micelles, solid lipid nanoparticles, liposomes, polymeric nanoparticles, SNEDDS, microgels…-, nanoemulsions have received a lot of attention for several reasons. For instance, microemulsions such as those used in our previous study are pseudo-ternary formulations comprising oil, aqueous media, a surfactant and a co-surfactant (ethanol) forming spontaneously and remaining thermodynamically stable, while nanoemulsions are a specialized drug delivery system composed of two non-miscible phases held together by surfactants, resulting in a stable and uniform solution. Moreover, nanoemulsions are composed of small particles (around 20 nm), which has the advantage to confer them low aggregability and gravitational separation, while allowing a marked increase in the bioavailability of lipophilic components (Mishra et al., 2024). Therefore, the aim of the present work was to develop DHA-loaded nanoemulsions to be used as a safe and stable formulation for intranasal administration. Because there is evidence that low-energy methods can produce droplets that are more uniform and smaller than those generated by high energy methods (Izquierdo et al., 2004; Ren et al., 2019), DHA was integrated into lipid nanocapsules using a low-energy, Phase Inversion Temperature (PIT) protocol (Izquierdo et al., 2004; Komaiko and McClements, 2016; Ren et al., 2019). Although there is evidence that metabolites formed through enzymatic or non-enzymatic DHA oxidation may play a role in modulating oxidative homeostasis in cells (Dyall et al., 2022), our previous observations indicated a gradual loss of efficiency between fresh microemulsions and those stored for several weeks at 4 °C (Zussy et al., 2022). This finding indicated that DHA oxidation may well contribute to the unpredictable effects of DHA supplementation and the frequent discrepancies observed in clinical studies. The stability of DHA in NEs was then assayed over a 5-months-period, with no loss being observed.

Moreover, as for microemulsions, a significant antioxidant capacity of NEs containing DHA was observed *in vitro*, with no decrease noted during storage at 4 °C. This stability was likely due to the presence of antioxidant agents such as tocopherol and rosemary extract titrated to 4 % carnosic acid in the DHA-rich Omegavie® batches. In addition, the presence of a dense and broad interfacial corona of Kolliphor® HS15 may also protect the DHA from oxidation. Kolliphor® HS15 was used at a high surfactant-oil ratio and its molecular weight is greater than some surfactants such as Tween® 80, classically used in the preparation of NEs (Nejadmansouri et al., 2016; Zhang et al., 2020a).

4.2. *Toxicity of nanoemulsions*

A pressing need exists for a delivery system that can bring bioactive molecules to the brain without disrupting the physiology and structure of the nasal epithelium or the BBB. DHA-NEs and vehicle-NEs did not significantly affect the viability of nasal epithelial cells at concentrations ranging from 0.01 % to 10 %. The loss of viability observed only at concentrations of 25 % and 50 % may be attributed to the high level of Kolliphor® HS15 in the culture medium. Cytotoxicity of Solutol® HS 15 in free form or in lipid nanocapsules was reported by Maupas *et al.* in HaCat cells (Maupas et al., 2011). A disruption of the cell membrane due to the amphiphilic properties of the non-ionic surfactant released from the nanocapsules was hypothesized.

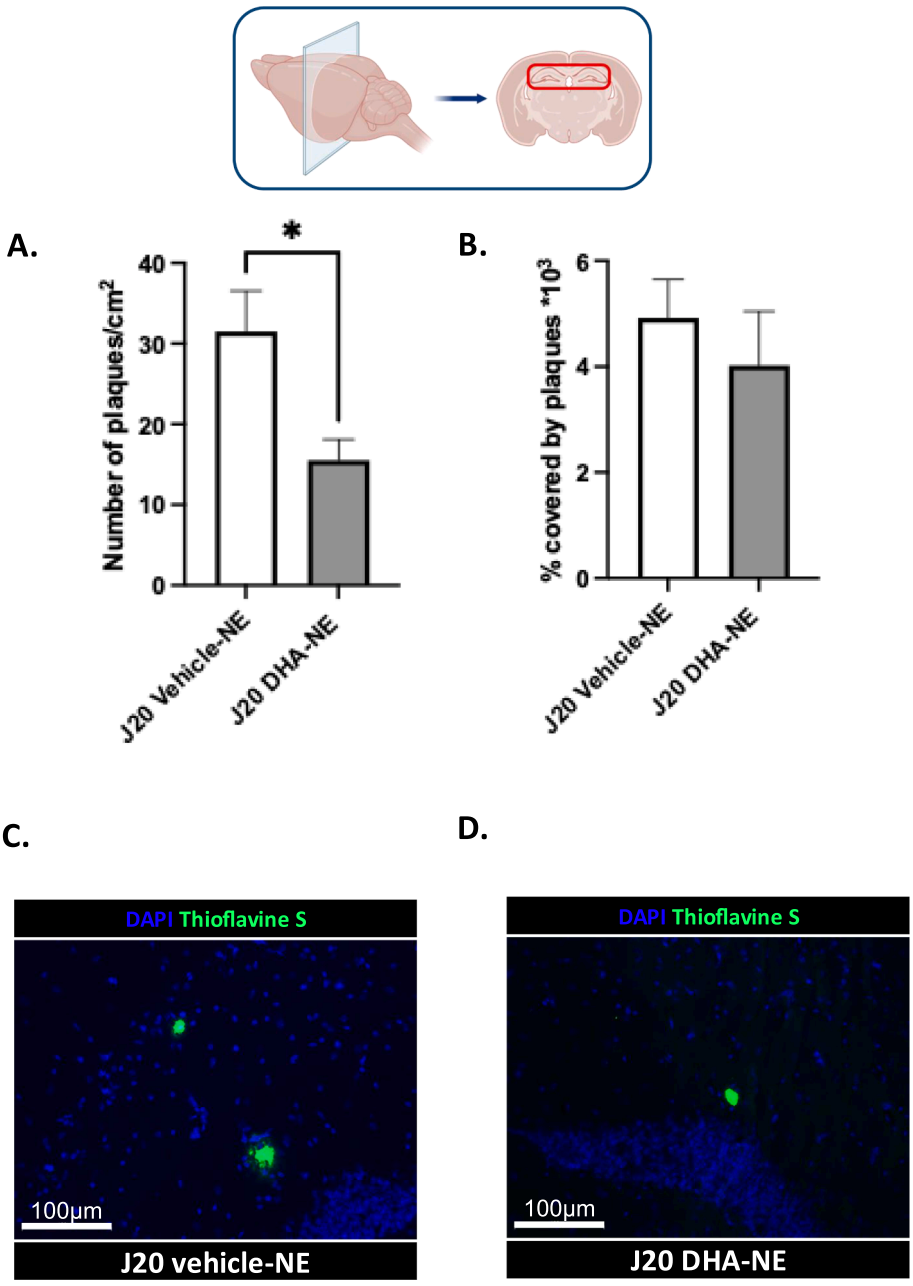

Fig. 6. Quantification of amyloid deposits in the hippocampus. Thioflavin T (ThT) staining was performed to quantify amyloid deposits in the hippocampus of brain sections from J20 mice treated with vehicle-NEs (n = 6) or DHA-NEs (n = 7) for 2 weeks. The number of ThT-positive aggregates is expressed as mean ± SEM/cm2 (**A**) and their surface area as mean ± SEM in percentage of the analyzed surface × 1,000 (**B**). (**C-D**) Representative images of amyloid plaques stained with ThT (in green) in the hippocampus of J20 mice treated with vehicle-NEs (left) or DHA-NEs (right). Aggregates were quantified using the Fiji software with 8–10 sections per animal. Statistical analysis was performed using an unpaired Student's *t* test, * $p < 0.05$.

4.3. Intranasal DHA and cognitive functions

We evaluated the effects of intranasal DHA-NEs treatment on cognitive loss in 6-months-old J20 mice, a model characterized by an early impairment of spatial memory and a depressive-like behavior (Mansuy et al., 2018; Quartey et al., 2019; Zussy et al., 2022). After a 2-week-treatment (5 days/week), the nesting, splash and Y-maze tests were performed. DHA-NEs treatment remarkably improved performance in all paradigms, indicating enhanced well-being and spatial working memory, as well as normalized depressive symptoms. This finding is in accordance with several studies in which dietary DHA supplementation was shown to counteract AD pathology in animal models (Badesso et al., 2022; Bie et al., 2021; Lim et al., 2005; Xiao et al., 2022), as well as cohort studies in which high DHA intakes were associated with a reduced risk of cognitive decline in middle-aged or older populations (Zhang et al., 2020b; Zhang et al., 2015). It is interesting to note that the dose of DHA used for the treatment in the present study was around 10 mg/kg, which is much lower than the doses typically tested for dietary supplementation. This lower dosage is important since it has been reported that high doses of antioxidants can lead to pro-oxidant effects (Véricel et al., 2003). In contrast to supplementation trials conducted in animal models, clinical studies did not allow to firmly conclude about the therapeutic potential of DHA for the prevention or treatment of AD. Our hypothesis is that this inconsistency can been explained by the long metabolic pathway DHA has to undergo before reaching the brain when administered by the oral dietary route

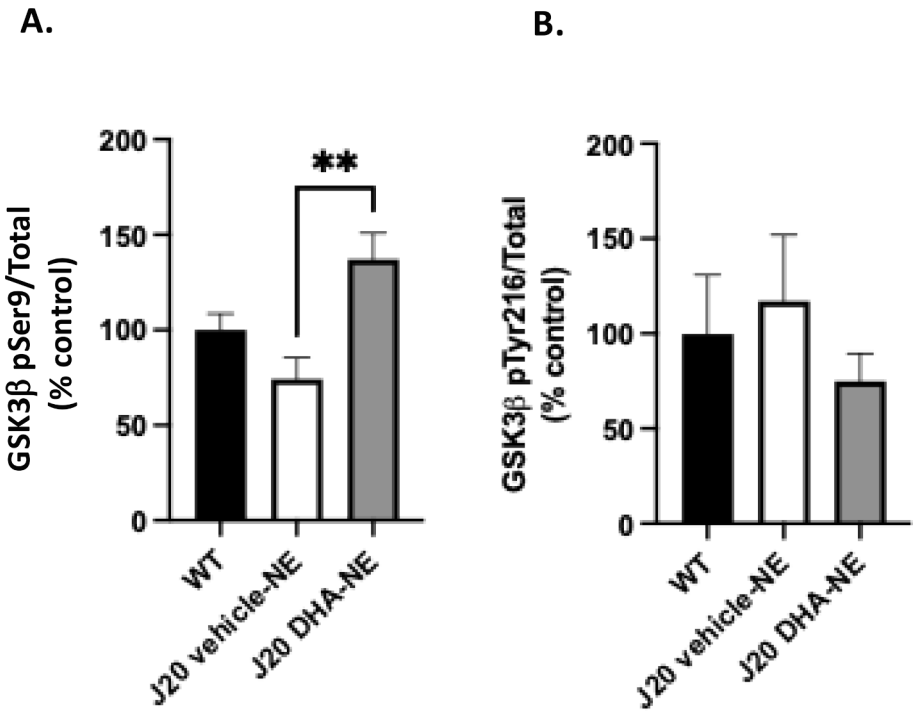

Fig. 7. Western Blot assessment of GSK3β phosphorylation. GSK3β phospho-epitope Tyr216 levels, which reflect its activation (**A**), and Ser9 levels, which reflect its inactivation (**B**) were quantified by immunoblot analysis of hippocampal lysates from WT and J20 mice. All results were normalized to total GSK3β protein levels and expressed as a percentage of the control (WT mice). Statistical analysis was performed using a one-way ANOVA followed by a Tukey post-hoc test, ** $p < 0.01$.

(Burckhardt et al., 2016). In particular, the BBB transport of DHA across the BBB is governed by several transporters, including fatty acid binding/transport proteins and Mfsd2a, whose activity seems to be modulated in animal models of AD. Indeed, Pan et al. demonstrated that the BBB transport of DHA is reduced in APP/PS1 mice, due to reduced expression of fatty acid binding protein. These mice are more vulnerable to DHA deficit, with reduced DHA access to the CNS that would contribute to impair both short-term spatial and recognition memory (Pan et al., 2015). Although there are no data available on the expression of these receptors in AD patients, it is noteworthy that the brain uptake of DHA has been reported to be inefficient in carriers of the E4 allele of apolipoprotein E, a known risk factor for sporadic AD (Tomaszewski et al., 2020). Therefore, we believe that using the intranasal route of administration, which allows to bypass of the BBB and provides direct access to the brain, is a very promising strategy that could make the difference to firmly demonstrate the potential of DHA to prevent cognitive loss in human subjects.

4.4. *Intranasal DHA, oxidative stress markers and neuroinflammation*

Isoprostanes (IsoPs) and neuroprostanes (NeuroPs) are unique series of prostaglandin-like compounds formed *in vivo through* a nonenzymatic mechanism involving the free radical-initiated peroxidation of arachidonic acid and DHA, respectively. These compounds are considered as markers of oxidative stress (Ahmed et al., 2020; Galano et al., 2017). It has been shown that Aβ aggregation generates reactive oxygen species (Hensley et al., 1994) and induces membrane lipid peroxidation (Mark et al., 1997). Moreover, previous studies have shown that lipid peroxidation can alter the proteolytic processing of the Aβ precursor protein (APP) in a manner that increases the production of Aβ, thereby initiating a vicious cycle. Specifically, oxidative lipid modification of the γ-secretase complex protein nicastrin enhances γ-secretase activity, resulting in increased Aβ production (Gwon et al., 2012). In 6-months-old vehicle-NEs-treated J20 mice, cerebral levels of 5-F_{2c}-isoprostanes and 10(*S*)-10-F_{4t}-neuroprostanes were not significantly different from those in WT mice, which may reflect compensatory overactivation of antioxidant defense mechanisms following Aβ peptide-induced toxicity. In DHA-NEs-treated J20 mice, cerebral levels of both markers were significantly lower than those measured in WT mice, suggesting an inhibitory effect of the treatment on lipid peroxidation and a potential for this therapeutic approach in protecting neurons against Aβ-induced degeneration. Thus, DHA-NEs would be expected to reduce the levels of Aβ, which represents a hypothesis that is consistent with our finding that amyloid deposits were significantly reduced in the hippocampus of DHA-NEs treated J20 mice.

Neuroinflammation plays an important role in the progression of AD, and omega-3 PUFAs are known to be involved in both the reduction and resolution of inflammation (Joffre et al., 2020). In the present study, an immunohistochemical analysis was conducted in the hippocampal region of brain tissue to characterize the effect of intranasal DHA-NEs treatment on astrogliosis and microgliosis. Although in our previous work no increase in GFAP, a marker of astrocyte activation, was observed in 3-months-old J20 mice, we here evidenced, in 6-months-old J20 mice compared to WT mice, that both astrocytes and microglia cell numbers were significantly increased in the dentate gyrus and CA3 regions of the hippocampus. Moreover, DHA-NEs treatment restored both neuroinflammatory markers to normal (WT) values. These results are in accordance with the well-documented anti-inflammatory properties of DHA, which may rely at least in part on the enzymatic generation of pro-resolving factors such as neuroprotectins and resolvins (Ponce et al., 2022). The pro-resolving and anti-inflammatory potential of resolvins in sporadic AD has been highlighted in recent studies (Anand et al., 2022).

4.5. *Intranasal DHA and amyloid deposition*

Cerebral amyloidosis results from several dynamic regulatory mechanisms. These mechanisms involve on the one hand the synthesis of Aβ peptides, with a competition between the non-amyloidogenic and amyloidogenic pathways governed by the enzymes ADAM10 and BACE1, respectively. On the other hand, Aβ peptide clearance that

mobilizes both peptidases (such as NEP and IDE) and removal transporters located at the BBB (LRP1, ABCB1, and RAGE). Amyloid deposition in the brain parenchyma can thus result from a disruption of the equilibrium between these pathways. In our previous work, we used young, 3-months-old J20 mice to focus on the impact of intranasal DHA administration on amyloid toxicity that occurs before amyloid deposition. Here, intranasal treatment with DHA-NEs was performed in 6-months-old J20 mice, which are known to exhibit amyloid deposits in the hippocampus (Masliah et al., 1996). A significant reduction in the number of amyloid plaques was observed following DHA-NEs treatment, with only a tendency towards reduced plaque surface, suggesting the treatment may inhibit the formation of new amyloid plaques. This is coherent with earlier findings showing that DHA-enriched diets can reduce amyloid burden in several murine AD models (Mett, 2021; Perez et al., 2010; Xiao et al., 2022).

DHA plays a crucial role as a modulator of gene expression *via* transcription factors, particularly peroxisome proliferator-activated receptors (PPARs) (Calder, 2015) and retinoid X receptors (RXRs) (Lengqvist et al., 2004; Urquiza et al., 2000). It has been shown that the PPARα-RXRα heterodimer can shift APP processing towards the non-amyloidogenic pathway in vivo by activating ADAM10 transcription (Corbett et al., 2015). Moreover, the activation of the PPARγ-RXRα heterodimer reduces β-secretase expression (Cao et al., 2016; Heneka et al., 2005; Sastre et al., 2006). This is consistent with the fact that DHA significantly increases the non-amyloidogenic APP processing pathway in cellular models (Eckert et al., 2011; Sahlin et al., 2007; Yang et al., 2011). Conversely, in the presence of oxidized lipids, a shift from the non-amyloidogenic to the amyloidogenic APP processing pathway occurs, leading to increased Aβ production. Indeed, it was reported that oxidized lipids elevate β-secretase activity both by upregulating BACE1 gene expression and by directly enhancing β-secretase activity (Grimm et al., 2016a; Tamagno et al., 2002).

Beyond APP processing and Aβ generation, omega-3 PUFAs are also clearly involved in brain Aβ clearance. Indeed, it has been reported that DHA up-regulates IDE levels (Du et al., 2010; Grimm et al., 2016b), and increases LRP1 expression and Aβ plasma levels through the activation of PPARγ-RXRα (Wang et al., 2016; Yan et al., 2020). Finally, the impact of DHA on amyloid deposition may be explained in part by its ability to destabilize Aβ fibrils, as recently reported by Gupta *et al.* (Gupta and Dasmahapatra, 2023).

In all cases, DHA levels are directly involved in the competition between the two APP processing pathways and in Aβ clearance. Our observation that amyloid deposition is reduced in DHA-NE-treated animals supports these findings.

4.6. Intranasal DHA and GSK3-beta activity

The GSK3β kinase plays a pivotal role in the pathology of AD, with abnormalities in its expression and activity have been reported in AD-related cell models, AD animal models and in AD/MCI patients (Hooper et al., 2008). Here, we observed a marked increase in GSK3β phosphorylation at Ser9 in DHA-NEs-treated J20 mice, suggesting a strong inhibition of its activity. Therefore, the beneficial effects of DHA-NEs observed in this study could be partially attributed to reduced GSK-3β activity. This assumption is supported by evidence that GSK-3β, which is abundantly expressed and highly active in AD, plays a number of negative roles in disease progression: while its role in tau phosphorylation is largely documented (Rankin et al., 2007), GSK-3β is also involved in Aβ formation from APP through various mechanisms, as well as in oxidative stress and neuroinflammation *via* its involvement in the Nrf2 and NF-κB signaling pathways (Hooper et al., 2008). Thus, it has been shown that GSK-3β can phosphorylate Nrf2 leading to its ubiquitination and degradation (Farr et al., 2014; Silva-Palacios et al., 2018), while its effects on NF-κB would be a consequence of Nrf2 inhibition and a subsequent increase in oxidative stress (Sun et al., 2021).

Interestingly, in the Fat-1 mouse model, which exhibits increased endogenous production of omega-3 fatty acids, an increase of GSK-3β phosphorylation at Ser9 was observed. This increase was shown to inhibit the Nrf2/Trx1 antioxidant pathway, which itself leads to activation of NF-κB and the inflammatory reaction (Zhu et al., 2022). In contrast, animals with global GSK-3β gene deletion have been reported to display a phenotype similar to those with decreased NF-κB activation (Patel and Woodgett, 2017). Furthermore, Moreira *et al.* demonstrated that omega-3 fatty acids deprivation is associated with increased GSK-3β activity, resulting in exacerbated cellular damage in a rat model of hippocampal ischemic insult (Moreira et al., 2010). The exact implication of reduced GSK-3β activity in the beneficial effect of DHA-NEs treatment will deserve further investigation.

5. Conclusion

In conclusion, we have demonstrated that intranasal administration of nanoformulated DHA protects it from oxidation and serves as an effective strategy to counteract oxidative stress, neuroinflammation, and amyloid plaque formation in a transgenic Alzheimer's disease model (J20 mice). These findings open the door to developing a novel approach for delivering DHA to the brain, offering potential for the prevention or treatment of this devastating disease.

Author contributions

LO, TU and CD designed the research; LO, TU, TZ, CZ, MV, NA, JMG, YP, CV, AB and CD performed the experiments; LO, TU, and CD analyzed data; LO, AB and CD wrote the manuscript; CZ, NA, TD, and LG corrected the manuscript. All authors read and approved the final manuscript.

CRediT authorship contribution statement

Léa Otaegui: Writing – original draft, Methodology, Data curation, Conceptualization. **Théo Urgin:** Formal analysis, Data curation, Conceptualization. **Taghrid Zaiter:** Formal analysis, Data curation. **Charleine Zussy:** Writing – review & editing, Methodology, Data curation. **Mathieu Vitalis:** Methodology, Formal analysis. **Yann Pellequer:** Methodology, Investigation, Formal analysis. **Niyazi Acar:** Methodology, Formal analysis, Data curation. **Claire Vigor:** Formal analysis, Data curation. **Jean-Marie Galano:** Methodology, Investigation, Formal analysis. **Thierry Durand:** Supervision, Investigation, Funding acquisition. **Laurent Givalois:** Writing – review & editing, Methodology, Investigation, Funding acquisition. **Arnaud Béduneau:** Writing – original draft, Methodology, Investigation, Conceptualization. **Catherine Desrumaux:** Writing – review & editing, Writing – original draft, Validation, Supervision, Funding acquisition, Formal analysis, Data curation, Conceptualization.

Declaration of competing interest

The authors declare that they have no known competing financial interests or personal relationships that could have appeared to influence the work reported in this paper.

Acknowledgements

The authors are thankful to the animal facility staff (CECEMA, University of Montpellier, France) for their daily assistance. This study was supported by INSERM, the University of Montpellier (France), and by a grant from the "Agence Nationale de la Recherche" (ANR) under the program "Investissements d'Avenir" (ANR-11-LABEX-0021-LipSTIC - CD). LO is supported by a PhD Grant from the University of Montpellier, France (CBS2 PhD program). LG was supported by grants from the "Agence Nationale de la Recherche" (ANR-AAP2022-R22102FF-Epi-NeurAge); the "Fondation pour la Recherche Médicale »

(MND2020030011477-OPA) and the University of Montpellier Program of Excellence (MUSE-AAP20REC-FRS09-GAiA).

Data availability

Data will be made available on request.

References

Acar, N., Berdeaux, O., Grégoire, S., Cabaret, S., Martine, L., Gain, P., Thuret, G., Creuzot-Garcher, C.P., Bron, A.M., Bretillon, L., 2012. Lipid composition of the human eye: are red blood cells a good mirror of retinal and optic nerve fatty acids? PLoS One 7, e35102. https://doi.org/10.1371/journal.pone.0035102.

Acar, N., Merle, B.M.J., Ajana, S., He, Z., Grégoire, S., Hejblum, B.P., Martine, L., Buaud, B., Bron, A.M., Creuzot-Garcher, C.P., Korobelnik, J., Berdeaux, O., Jacqmin-Gadda, H., Bretillon, L., Delcourt, C., for the Biomarkers of Lipid Status And metabolism in Retinal ageing (BLISAR) Study Group, Acar, N., Ajana, S., Berdeaux, O., Bretillon, L., Bron, A., Buaud, B., Cabaret, S., Gain, P., Cougnard-Grégoire, A., Creuzot-Garcher, C., Delcourt, C., Delyfer, M., Féart, C., Febvret, V., Grégoire, S., He, Z., Korobelnik, J., Martine, L., MJ Merle, B., Thuret, G., Vaysse, C., 2021. Predicting the retinal content in omega-3 fatty acids for age-related macular-degeneration. Clinical and Translational Medicine 11 (7), e404. https://doi.org/10.1002/ctm2.404.

Ahmed, O.S., Galano, J.-M., Pavlickova, T., Revol-Cavalier, J., Vigor, C., Lee, J.-C.-Y., Oger, C., Durand, T., 2020. Moving forward with isoprostanes, neuroprostanes and phytoprostanes: where are we now? Essays Biochem. 64, 463–484. https://doi.org/10.1042/EBC20190096.

Anand, S., Azam Ansari, M., Kumaraswamy Sukrutha, S., Alomary, M.N., Anwar Khan, A., Elderdery, A.Y., 2022. Resolvins lipid mediators: potential therapeutic targets in Alzheimer and Parkinson disease. Neuroscience 507, 139–148. https://doi.org/10.1016/j.neuroscience.2022.11.001.

Arvanitakis, Z., 2024. The need to better understand aging and risk factors for dementia. Front. Dement. 2, 1346281. https://doi.org/10.3389/frdem.2023.1346281.

Badesso, S., Cartas-Cejudo, P., Espelosin, M., Santamaria, E., Cuadrado-Tejedor, M., Garcia-Osta, A., 2022. Docosahexaenoic acid ameliorates contextual fear memory deficits in the Tg2576 Alzheimer's disease mouse model: cellular and molecular correlates. Pharmaceutics 15, 82. https://doi.org/10.3390/pharmaceutics15010082.

Bie, N., Li, J., Li, C., Lian, R., Qin, L., Wang, C., 2021. Protective effect and mechanism of docosahexaenoic acid on the cognitive function in female APP/PS1 mice. Food Funct. 12, 11435–11448. https://doi.org/10.1039/D1FO01922H.

Burckhardt, M., Herke, M., Wustmann, T., Watzke, S., Langer, G., Fink, A., 2016. Omega-3 fatty acids for the treatment of dementia. Cochrane Database Syst. Rev. https://doi.org/10.1002/14651858.CD009002.pub3.

Calder, P.C., 2015. Marine omega-3 fatty acids and inflammatory processes: effects, mechanisms and clinical relevance. Biochimica et Biophysica Acta (BBA) – Mol. Cell Bio. Lipids 1851, 469–484. https://doi.org/10.1016/j.bbalip.2014.08.010.

Cao, G., Su, P., Zhang, S., Guo, L., Zhang, H., Liang, Y., Qin, C., Zhang, W., 2016. Ginsenoside Re reduces Aβ production by activating PPARγ to inhibit BACE1 in N2a/APP695 cells. Eur. J. Pharmacol. 793, 101–108. https://doi.org/10.1016/j.ejphar.2016.11.006.

Cole, G.M., Frautschy, S.A., 2006. Docosahexaenoic acid protects from amyloid and dendritic pathology in an Alzheimer's disease mouse model. Nutr. Health 18, 249–259. https://doi.org/10.1177/026010600601800307.

Corbett, G.T., Gonzalez, F.J., Pahan, K., 2015. Activation of peroxisome proliferator-activated receptor α stimulates ADAM10-mediated proteolysis of APP. PNAS 112, 8445–8450. https://doi.org/10.1073/pnas.1504890112.

Desrumaux, C., Pisoni, A., Meunier, J., Deckert, V., Athias, A., Perrier, V., Villard, V., Lagrost, L., Verdier, J.-M., Maurice, T., 2013. Increased amyloid-β peptide-induced memory deficits in phospholipid transfer protein (PLTP) gene knockout mice. Neuropsychopharmacol 38, 817–825. https://doi.org/10.1038/npp.2012.247.

Dighriri, I.M., Alsubaie, A.M., Hakami, F.M., Hamithi, D.M., Alshekh, M.M., Khobrani, F. A., Dalak, F.E., Hakami, A.A., Alsueaadi, E.H., Alsaawi, L.S., Alshammari, S.F., Alqahtani, A.S., Alawi, I.A., Aljuaid, A.A., Tawhari, M.Q., 2022. Effects of omega-3 polyunsaturated fatty acids on brain functions: a systematic review. Cureus. https://doi.org/10.7759/cureus.30091.

Du, J., Zhang, L., Liu, S., Wang, Z., 2010. Palmitic acid and docosahexaenoic acid opposingly regulate the expression of insulin-degrading enzyme in neurons. Pharmazie 65, 231–232.

Dyall, S.C., Balas, L., Bazan, N.G., Brenna, J.T., Chiang, N., Da Costa Souza, F., Dalli, J., Durand, T., Galano, J.-M., Lein, P.J., Serhan, C.N., Taha, A.Y., 2022. Polyunsaturated fatty acids and fatty acid-derived lipid mediators: Recent advances in the understanding of their biosynthesis, structures, and functions. Prog. Lipid Res. 86, 101165. https://doi.org/10.1016/j.plipres.2022.101165.

Eckert, G.P., Chang, S., Eckmann, J., Copanaki, E., Hagl, S., Hener, U., Müller, W.E., Kögel, D., 2011. Liposome-incorporated DHA increases neuronal survival by enhancing non-amyloidogenic APP processing. Biochimica et Biophysica Acta (BBA) - Biomembranes 1808, 236–243. https://doi.org/10.1016/j.bbamem.2010.10.014.

Erdő, F., Bors, L.A., Farkas, D., Bajza, Á., Gizurarson, S., 2018. Evaluation of intranasal delivery route of drug administration for brain targeting. Brain Res. Bull. 143, 155–170. https://doi.org/10.1016/j.brainresbull.2018.10.009.

Farr, S.A., Ripley, J.L., Sultana, R., Zhang, Z., Niehoff, M.L., Platt, T.L., Murphy, M.P., Morley, J.E., Kumar, V., Butterfield, D.A., 2014. Antisense oligonucleotide against GSK-3β in brain of SAMP8 mice improves learning and memory and decreases oxidative stress: involvement of transcription factor Nrf2 and implications for Alzheimer disease. Free Radic. Biol. Med. 67, 387–395. https://doi.org/10.1016/j.freeradbiomed.2013.11.014.

Folch, J., Lees, M., Sloane Stanley, G.H., 1957. A simple method for the isolation and purification of total lipides from animal tissues. J. Biol. Chem. 226, 497–509.

Galano, J.-M., Lee, Y.Y., Oger, C., Vigor, C., Vercauteren, J., Durand, T., Giera, M., Lee, J.-C.-Y., 2017. Isoprostanes, neuroprostanes and phytoprostanes: an overview of 25 years of research in chemistry and biology. Prog. Lipid Res. 68, 83–108. https://doi.org/10.1016/j.plipres.2017.09.004.

Gao, Q., Niti, M., Feng, L., Yap, K.B., Ng, T.P., 2011. Omega-3 polyunsaturated fatty acid supplements and cognitive decline: Singapore longitudinal aging studies. J. Nutr. Health Aging 15, 32–35. https://doi.org/10.1007/s12603-011-0010-z.

Gillette Guyonnet, S., Abellan Van Kan, G., Andrieu, S., Barberger Gateau, P., Berr, C., Bonnefoy, M., Dartigues, J.F., de Groot, L., Ferry, M., Galan, P., Hercberg, S., Jeandel, C., Morris, M.C., Nourhashemi, F., Payette, H., Poulain, J.P., Portet, F., Roussel, A.M., Ritz, P., Rolland, Y., Vellas, B., 2007. IANA task force on nutrition and cognitive decline with aging. J. Nutr. Health Aging 11, 132–152.

Grimm, M.O.W., Haupenthal, V.J., Mett, J., Stahlmann, C.P., Blümel, T., Mylonas, N.T., Endres, K., Grimm, H.S., Hartmann, T., 2016a. Oxidized docosahexaenoic acid species and lipid peroxidation products increase amyloidogenic amyloid precursor protein processing. Neurodegener Dis 16, 44–54. https://doi.org/10.1159/000440839.

Grimm, M.O.W., Mett, J., Stahlmann, C.P., Haupenthal, V.J., Blümel, T., Stötzel, H., Grimm, H.S., Hartmann, T., 2016b. Eicosapentaenoic acid and docosahexaenoic acid increase the degradation of amyloid-β by affecting insulin-degrading enzyme. Biochem. Cell Biol. 94, 534–542. https://doi.org/10.1139/bcb-2015-0149.

Gupta, S., Dasmahapatra, A.K., 2023. Destabilization of Aβ fibrils by omega-3 polyunsaturated fatty acids: a molecular dynamics study. J. Biomol. Struct. Dyn. 41, 581–598. https://doi.org/10.1080/07391102.2021.2009915.

Gwon, A., Park, J., Arumugam, T.V., Kwon, Y., Chan, S.L., Kim, S.-H., Baik, S., Yang, S., Yun, Y., Choi, Y., Kim, S., Tang, S., Hyun, D., Cheng, A., Dann, C.E., Bernier, M., Lee, J., Markesbery, W.R., Mattson, M.P., Jo, D., 2012. Oxidative lipid modification of nicastrin enhances amyloidogenic γ-secretase activity in Alzheimer's disease. Aging Cell 11, 559–568. https://doi.org/10.1111/j.1474-9726.2012.00817.x.

Hallschmid, M., 2021. Intranasal insulin for Alzheimer's disease. CNS Drugs 35, 21–37. https://doi.org/10.1007/s40263-020-00781-x.

Heneka, M.T., Sastre, M., Dumitrescu-Ozimek, L., Hanke, A., Dewachter, I., Kuiperi, C., O'Banion, K., Klockgether, T., Van Leuven, F., Landreth, G.E., 2005. Acute treatment with the PPARγ agonist pioglitazone and ibuprofen reduces glial inflammation and Aβ1–42 levels in APPV717I transgenic mice. Brain 128, 1442–1453. https://doi.org/10.1093/brain/awh452.

Hensley, K., Carney, J.M., Mattson, M.P., Aksenova, M., Harris, M., Wu, J.F., Floyd, R.A., Butterfield, D.A., 1994. A model for beta-amyloid aggregation and neurotoxicity based on free radical generation by the peptide: relevance to Alzheimer disease. PNAS 91, 3270–3274. https://doi.org/10.1073/pnas.91.8.3270.

Hess, S.E., Rohr, S., Dufour, B.D., Gaskill, B.N., Pajor, E.A., Garner, J.P., 2008. Home improvement: C57BL/6J mice given more naturalistic nesting materials build better nests. J. Am. Assoc. Lab. Anim. Sci. 47, 25–31.

Hooijmans, C.R., Van der Zee, C.E.E.M., Dederen, P.J., Brouwer, K.M., Reijmer, Y.D., van Groen, T., Broersen, L.M., Lütjohann, D., Heerschap, A., Kiliaan, A.J., 2009. DHA and cholesterol containing diets influence Alzheimer-like pathology, cognition and cerebral vasculature in APPswe/PS1dE9 mice. Neurobiol. Dis. 33, 482–498. https://doi.org/10.1016/j.nbd.2008.12.002.

Hooper, C., Killick, R., Lovestone, S., 2008. The GSK3 hypothesis of Alzheimer's disease: GSK3 and Alzheimer's disease. J. Neurochem. 104, 1433–1439. https://doi.org/10.1111/j.1471-4159.2007.05194.x.

Huang, D., Ou, B., Hampsch-Woodill, M., Flanagan, J.A., Prior, R.L., 2002. High-throughput assay of oxygen radical absorbance capacity (ORAC) using a multichannel liquid handling system coupled with a microplate fluorescence reader in 96-well format. J. Agric. Food Chem. 50, 4437–4444. https://doi.org/10.1021/jf0201529.

Izquierdo, P., Esquena, J., Tadros, T.F., Dederen, J.C., Feng, J., Garcia-Celma, M.J., Azemar, N., Solans, C., 2004. Phase behavior and nano-emulsion formation by the phase inversion temperature method. Langmuir 20, 6594–6598. https://doi.org/10.1021/la049566h.

Jamoussi, Y., Zaiter, T., Desrumaux, C., Acar, N., Pellequer, Y., Béduneau, A., 2021. Investigation of the spontaneous nanoemulsification process with medium- and long-chain triglycerides. Colloids Surf. B Biointerfaces 197, 111432. https://doi.org/10.1016/j.colsurfb.2020.111432.

Joffre, C., Dinel, A.-L., Chataigner, M., Pallet, V., Layé, S., 2020. n-3 polyunsaturated fatty acids and their derivates reduce neuroinflammation during aging. Nutrients 12, 647. https://doi.org/10.3390/nu12030647.

Komaiko, J.S., McClements, D.J., 2016. Formation of food-grade nanoemulsions using low-energy preparation methods: a review of available methods. Comp. Rev. Food Sci. Food Safe 15, 331–352. https://doi.org/10.1111/1541-4337.12189.

Kong, C.H., Park, K., Kim, D.Y., Kim, J.Y., Kang, W.C., Jeon, M., Min, J.W., Lee, W.H., Jung, S.Y., Ryu, J.H., 2023. Effects of oleanolic acid and ursolic acid on depression-like behaviors induced by maternal separation in mice. Eur. J. Pharmacol. 956, 175954. https://doi.org/10.1016/j.ejphar.2023.175954.

Kumar, H., Mishra, G., Sharma, A.K., Gothwal, A., Kesharwani, P., Gupta, U., 2018. Intranasal drug delivery: a non-invasive approach for the better delivery of neurotherapeutics. PNT 5. https://doi.org/10.2174/2211738505666170515113936.

Lafon, P.-A., Wang, Y., Arango-Lievano, M., Torrent, J., Salvador-Prince, L., Mansuy, M., Mestre-Francès, N., Givalois, L., Liu, J., Mercader, J.V., Jeanneteau, F.,

Desrumaux, C., Perrier, V., 2020. Fungicide residues exposure and β-amyloid aggregation in a mouse model of Alzheimer's disease. Environ. Health Perspect. 128, 017011. https://doi.org/10.1289/EHP5550.

Lengqvist, J., Mata De Urquiza, A., Bergman, A.-C., Willson, T.M., Sjövall, J., Perlmann, T., Griffiths, W.J., 2004. Polyunsaturated fatty acids including docosahexaenoic and arachidonic acid bind to the retinoid X receptor α ligand-binding domain. Mol. Cell. Proteomics 3, 692–703. https://doi.org/10.1074/mcp.M400003-MCP200.

Lim, G.P., Calon, F., Morihara, T., Yang, F., Teter, B., Ubeda, O., Salem, N., Frautschy, S. A., Cole, G.M., 2005. A diet enriched with the omega-3 fatty acid docosahexaenoic acid reduces amyloid burden in an aged Alzheimer mouse model. J. Neurosci. 25, 3032–3040. https://doi.org/10.1523/JNEUROSCI.4225-04.2005.

Liu, Y., Liang, Y., Yuhong, J., Xin, P., Han, J.L., Du, Y., Yu, X., Zhu, R., Zhang, M., Chen, W., Ma, Y., 2024. Advances in nanotechnology for enhancing the solubility and bioavailability of poorly soluble drugs. DDDT 18, 1469–1495. https://doi.org/10.2147/DDDT.S447496.

Lo Van, A., Sakayori, N., Hachem, M., Belkouch, M., Picq, M., Lagarde, M., Osumi, N., Bernoud-Hubac, N., 2016. Mechanisms of DHA transport to the brain and potential therapy to neurodegenerative diseases. Biochimie 130, 163–167. https://doi.org/10.1016/j.biochi.2016.07.011.

Maclean, C.H., Issa, A.M., Newberry, S.J., Mojica, W.A., Morton, S.C., Garland, R.H., Hilton, L.G., Traina, S.B., Shekelle, P.G., 2005. Effects of omega-3 fatty acids on cognitive function with aging, dementia, and neurological diseases. Evid. Rep. Technol. Assess. (Summ.) 1–3.

Mallick, R., Basak, S., Duttaroy, A.K., 2019. Docosahexaenoic acid, 22:6n-3: its roles in the structure and function of the brain. Int. J. Dev. Neurosci. 79, 21–31. https://doi.org/10.1016/j.ijdevneu.2019.10.004.

Mansuy, M., Baille, S., Canet, G., Borie, A., Cohen-Solal, C., Vignes, M., Perrier, V., Chevallier, N., Le Guern, N., Deckert, V., Lagrost, L., Givalois, L., Desrumaux, C., 2018. Deletion of plasma *Phospholipid Transfer Protein (PLTP)* increases microglial phagocytosis and reduces cerebral amyloid-β deposition in the J20 mouse model of Alzheimer's disease. Oncotarget 9, 19688–19703. https://doi.org/10.18632/oncotarget.24802.

Mark, R.J., Pang, Z., Geddes, J.W., Uchida, K., Mattson, M.P., 1997. Amyloid β-peptide impairs glucose transport in hippocampal and cortical neurons: involvement of membrane lipid peroxidation. J. Neurosci. 17, 1046–1054. https://doi.org/10.1523/JNEUROSCI.17-03-01046.1997.

Masliah, E., Sisk, A., Mallory, M., Mucke, L., Schenk, D., Games, D., 1996. Comparison of neurodegenerative pathology in transgenic mice overexpressing V717F β-amyloid precursor protein and Alzheimer's disease. J. Neurosci. 16, 5795–5811. https://doi.org/10.1523/JNEUROSCI.16-18-05795.1996.

Maupas, C., Moulari, B., Béduneau, A., Lamprecht, A., Pellequer, Y., 2011. Surfactant dependent toxicity of lipid nanocapsules in HaCaT cells. Int. J. Pharm. 411, 136–141. https://doi.org/10.1016/j.ijpharm.2011.03.056.

Mett, J., 2021. The impact of medium chain and polyunsaturated ω-3-fatty acids on amyloid-β deposition, oxidative stress and metabolic dysfunction associated with Alzheimer's disease. Antioxidants 10, 1991. https://doi.org/10.3390/antiox10121991.

Mishra, I., Mishra, R., Dubey, A., Dhakad, P.K., 2024. A Perspective on various facets of nanoemulsions and its commercial utilities. Assay Drug Dev. Technol. 22, 97–117. https://doi.org/10.1089/adt.2023.042.

Mohajeri, M.H., Troesch, B., Weber, P., 2015. Inadequate supply of vitamins and DHA in the elderly: implications for brain aging and Alzheimer-type dementia. Nutrition 31, 261–275. https://doi.org/10.1016/j.nut.2014.06.016.

Moreira, J.D., Knorr, L., Thomazi, A.P., Simão, F., Battú, C., Oses, J.P., Gottfried, C., Wofchuk, S., Salbego, C., Souza, D.O., Perry, M.L.S., Vinadé, L., 2010. Dietary omega-3 fatty acids attenuate cellular damage after a hippocampal ischemic insult in adult rats. J. Nutr. Biochem. 21, 351–356. https://doi.org/10.1016/j.jnutbio.2009.01.013.

Moretti, M., Colla, A., de Oliveira Balen, G., dos Santos, D.B., Budni, J., de Freitas, A.E., Farina, M., Severo Rodrigues, A.L., 2012. Ascorbic acid treatment, similarly to fluoxetine, reverses depressive-like behavior and brain oxidative damage induced by chronic unpredictable stress. J. Psychiatr. Res. 46, 331–340. https://doi.org/10.1016/j.jpsychires.2011.11.009.

Morrison, W.R., Smith, L.M., 1964. Preparation of fatty acid methyl esters and dimethylacetals from lipids with boron fluoride–methanol. J. Lipid Res. 5, 600–608.

Nejadmansouri, M., Hosseini, S.M.H., Niakosari, M., Yousefi, G.H., Golmakani, M.T., 2016. Physicochemical properties and oxidative stability of fish oil nanoemulsions as affected by hydrophilic lipophilic balance, surfactant to oil ratio and storage temperature. Colloids Surf. A Physicochem. Eng. Asp. 506, 821–832. https://doi.org/10.1016/j.colsurfa.2016.07.075.

Oster, T., Pillot, T., 2010. Docosahexaenoic acid and synaptic protection in Alzheimer's disease mice. Biochimica et Biophysica Acta (BBA) – Mol. Cell Bio. Lipids 1801, 791–798. https://doi.org/10.1016/j.bbalip.2010.02.011.

Pan, Y., Khalil, H., Nicolazzo, J., 2015. The impact of docosahexaenoic acid on Alzheimer's disease: is there a role of the blood-brain barrier? CCP 10, 222–241. https://doi.org/10.2174/1574884710031508201515532.

Patel, P., Woodgett, J.R., 2017. Glycogen synthase kinase 3: a kinase for all pathways? Current topics in developmental biology 123, 277–302. https://doi.org/10.1016/bs.ctdb.2016.11.011.

Perez, S.E., Berg, B.M., Moore, K.A., He, B., Counts, S.E., Fritz, J.J., Hu, Y., Lazarov, O., Lah, J.J., Mufson, E.J., 2010. DHA diet reduces AD pathology in young APPswe/PS1ΔE9 transgenic mice: possible gender effects. J. Neurosci. Res. 88, 1026–1040. https://doi.org/10.1002/jnr.22266.

Plourde, M., Cunnane, S.C., 2007. Extremely limited synthesis of long chain polyunsaturates in adults: implications for their dietary essentiality and use as supplements. Appl. Physiol. Nutr. Metab. 32, 619–634. https://doi.org/10.1139/H07-034.

Plourde, M., Fortier, M., Vandal, M., Tremblay-Mercier, J., Freemantle, E., Bégin, M., Pifferi, F., Cunnane, S.C., 2007. Unresolved issues in the link between docosahexaenoic acid and Alzheimer's disease. Prostaglandins Leukot. Essent. Fat. Acids 77, 301–308. https://doi.org/10.1016/j.plefa.2007.10.024.

Ponce, J., Ulu, A., Hanson, C., Cameron-Smith, E., Bertoni, J., Wuebker, J., Fisher, A., Siu, K.-C., Marmelat, V., Adamec, J., Bhatti, D., 2022. Role of specialized pro-resolving mediators in reducing neuroinflammation in neurodegenerative disorders. Front. Aging Neurosci. 14, 780811. https://doi.org/10.3389/fnagi.2022.780811.

Prasad, M.R., Lovell, M.A., Yatin, M., Dhillon, H., Markesbery, W.R., 1998. No title found. Neurochem. Res. 23, 81–88. https://doi.org/10.1023/A:1022457605436.

Quartey, M.O., Nyarko, J.N.K., Pennington, P.R., Heistad, R.M., Chaharyn, B.M., Wei, Z., Bainbridge, D., Baker, G.B., Mousseau, D.D., 2019. Age- and sex-dependent profiles of APP fragments and key secretases align with changes in despair-like behavior and cognition in young APPSwe/Ind mice. Biochem. Biophys. Res. Commun. 511, 454–459. https://doi.org/10.1016/j.bbrc.2019.02.083.

Rahman, M.A., Rahman, M.S., Uddin, M.J., Mamum-Or-Rashid, A.N.M., Pang, M.-G., Rhim, H., 2020. Emerging risk of environmental factors: insight mechanisms of Alzheimer's diseases. Environ. Sci. Pollut. Res. 27, 44659–44672. https://doi.org/10.1007/s11356-020-08243-z.

Rankin, C.A., Sun, Q., Gamblin, T.C., 2007. Tau phosphorylation by GSK-3β promotes tangle-like filament morphology. Mol. Neurodegeneration 2, 12. https://doi.org/10.1186/1750-1326-2-12.

Rathee, S., Sen, D., Pandey, V., Jain, S.K., 2024. Advances in understanding and managing Alzheimer's disease: from pathophysiology to innovative therapeutic strategies. CDT 25. https://doi.org/10.2174/0113894501320096240627071400.

Ren, G., Sun, Z., Wang, Z., Zheng, X., Xu, Z., Sun, D., 2019. Nanoemulsion formation by the phase inversion temperature method using polyoxypropylene surfactants. J. Colloid Interface Sci. 540, 177–184. https://doi.org/10.1016/j.jcis.2019.01.018.

Roy, J., Vigor, C., Vercauteren, J., Reversat, G., Zhou, B., Surget, A., Larroquet, L., Lanuque, A., Sandres, F., Terrier, F., Oger, C., Galano, J.-M., Corraze, G., Durand, T., 2020. Characterization and modulation of brain lipids content of rainbow trout fed with 100% plant based diet rich in omega-3 long chain polyunsaturated fatty acids DHA and EPA. Biochimie 178, 137–147. https://doi.org/10.1016/j.biochi.2020.06.010.

Sahlin, C., Pettersson, F.E., Nilsson, L.N.G., Lannfelt, L., Johansson, A., 2007. Docosahexaenoic acid stimulates non-amyloidogenic APP processing resulting in reduced Aβ levels in cellular models of Alzheimer's disease. Eur J of Neuroscience 26, 882–889. https://doi.org/10.1111/j.1460-9568.2007.05719.x.

Sastre, M., Dewachter, I., Rossner, S., Bogdanovic, N., Rosen, E., Borghgraef, P., Evert, B. O., Dumitrescu-Ozimek, L., Thal, D.R., Landreth, G., Walter, J., Klockgether, T., Van Leuven, F., Heneka, M.T., 2006. Nonsteroidal anti-inflammatory drugs repress β-secretase gene promoter activity by the activation of PPARγ. PNAS 103, 443–448. https://doi.org/10.1073/pnas.0503839103.

Silva-Palacios, A., Ostolga-Chavarría, M., Zazueta, C., Königsberg, M., 2018. Nrf2: molecular and epigenetic regulation during aging. Ageing Res. Rev. 47, 31–40. https://doi.org/10.1016/j.arr.2018.06.003.

Sun, C.-P., Zhang, X.-Y., Zhou, J.-J., Huo, X.-K., Yu, Z.-L., Morisseau, C., Hammock, B.D., Ma, X.-C., 2021. Inhibition of sEH via stabilizing the level of EETs alleviated Alzheimer's disease through GSK3β signaling pathway. Food Chem. Toxicol. 156, 112516. https://doi.org/10.1016/j.fct.2021.112516.

Tamagno, E., Bardini, P., Obbili, A., Vitali, A., Borghi, R., Zaccheo, D., Pronzato, M.A., Danni, O., Smith, M.A., Perry, G., Tabaton, M., 2002. Oxidative stress increases expression and activity of BACE in NT2 neurons. Neurobiol. Dis. 10, 279–288. https://doi.org/10.1006/nbdi.2002.0515.

Teng, E., Taylor, K., Bilousova, T., Weiland, D., Pham, T., Zuo, X., Yang, F., Chen, P.-P., Glabe, C.G., Takacs, A., Hoffman, D.R., Frautschy, S.A., Cole, G.M., 2015. Dietary DHA supplementation in an APP/PS1 transgenic rat model of AD reduces behavioral and Aβ pathology and modulates Aβ oligomerization. Neurobiol. Dis. 82, 552–560. https://doi.org/10.1016/j.nbd.2015.09.002.

Tomaszewski, N., He, X., Solomon, V., Lee, M., Mack, W.J., Quinn, J.F., Braskie, M.N., Yassine, H.N., 2020. Effect of APOE genotype on plasma docosahexaenoic acid (DHA), eicosapentaenoic acid, arachidonic acid, and hippocampal volume in the Alzheimer's disease cooperative study-sponsored DHA clinical trial. JAD 74, 975–990. https://doi.org/10.3233/JAD-191017.

Urquiza, A.M.D., Liu, S., Sjöberg, M., Zetterström, R.H., Griffiths, W., Sjövall, J., Perlmann, T., 2000. Docosahexaenoic acid, a ligand for the retinoid X receptor in mouse brain. Science 290, 2140–2144. https://doi.org/10.1126/science.290.5499.2140.

Véricel, E., Polette, A., Bacot, S., Calzada, C., Lagarde, M., 2003. Pro- and antioxidant activities of docosahexaenoic acid on human blood platelets: *DHA and platelet redox status*. J. Thromb. Haemost. 1, 566–572. https://doi.org/10.1046/j.1538-7836.2003.00076.x.

von Schacky, C., 2021. Importance of EPA and DHA blood levels in brain structure and function. Nutrients 13, 1074. https://doi.org/10.3390/nu13041074.

Wang, H., Chen, F., Zhong, K.L., Tang, S.S., Hu, M., Long, Y., Miao, M.X., Liao, J.M., Sun, H.B., Hong, H., 2016. PPARγ agonists regulate bidirectional transport of amyloid-β across the blood–brain barrier and hippocampus plasticity in *db / db* mice. British J. Pharmacol. 173, 372–385. https://doi.org/10.1111/bph.13378.

Willner, P., 2005. Chronic mild stress (CMS) revisited: consistency and behavioural-neurobiological concordance in the effects of CMS. Neuropsychobiology 52, 90–110. https://doi.org/10.1159/000087097.

Witting, L.A., Horwitt, M.K., 1964. Effect of degree of fatty acid unsaturation in tocopherol deficiency-induced creatinuria. J. Nutr. 82, 19–33. https://doi.org/10.1093/jn/82.1.19.

Xiao, M., Xiang, W., Chen, Y., Peng, N., Du, X., Lu, S., Zuo, Y., Li, B., Hu, Y., Li, X., 2022. DHA ameliorates cognitive ability, reduces amyloid deposition, and nerve fiber production in Alzheimer's disease. Front. Nutr. 9, 852433. https://doi.org/10.3389/fnut.2022.852433.

Yan, L., Xie, Y., Satyanarayanan, S.K., Zeng, H., Liu, Q., Huang, M., Ma, Y., Wan, J.-B., Yao, X., Su, K.-P., Su, H., 2020. Omega-3 polyunsaturated fatty acids promote brain-to-blood clearance of β-Amyloid in a mouse model with Alzheimer's disease. Brain Behav. Immun. 85, 35–45. https://doi.org/10.1016/j.bbi.2019.05.033.

Yang, X., Sheng, W., Sun, G.Y., Lee, J.-C.-M., 2011. Effects of fatty acid unsaturation numbers on membrane fluidity and α-secretase-dependent amyloid precursor protein processing. Neurochem. Int. 58, 321–329. https://doi.org/10.1016/j.neuint.2010.12.004.

Zhang, Y., Chen, J., Qiu, J., Li, Y., Wang, J., Jiao, J., 2015. Intakes of fish and polyunsaturated fatty acids and mild-to-severe cognitive impairment risks: a dose-response meta-analysis of 21 cohort studies1–3. Am. J. Clin. Nutr. 103, 330–340. https://doi.org/10.3945/ajcn.115.124081.

Zhang, L., Han, C., Liu, M., Yang, H., Zhang, F., Liu, B., Meng, X., 2020a. The formation, stability of DHA/EPA nanoemulsion prepared by emulsion phase inversion method and its application in apple juice. Food Res. Int. 133, 109132. https://doi.org/10.1016/j.foodres.2020.109132.

Zhang, T., Han, X., Zhang, X., Chen, Z., Mi, Y., Gou, X., 2020b. Dietary fatty acid factors in Alzheimer's disease: a review. JAD 78, 887–904. https://doi.org/10.3233/JAD-200558.

Zhao, Z.Q., Chen, B.Z., Zhang, X.P., Zheng, H., Guo, X.D., 2021. An update on the routes for the delivery of donepezil. Mol. Pharm. 18, 2482–2494. https://doi.org/10.1021/acs.molpharmaceut.1c00290.

Zhu, P., Zhang, J.-J., Cen, Y., Yang, Y., Wang, F., Gu, K.-P., Yang, H.-T., Wang, Y.-Z., Zou, Z.-Q., 2022. High endogenously synthesized N-3 polyunsaturated fatty acids in fat-1 mice attenuate high-fat diet-induced insulin resistance by inhibiting NLRP3 inflammasome activation via Akt/GSK-3β/TXNIP pathway. Molecules 27, 6384. https://doi.org/10.3390/molecules27196384.

Zussy, C., John, R., Urgin, T., Otaegui, L., Vigor, C., Acar, N., Canet, G., Vitalis, M., Morin, F., Planel, E., Oger, C., Durand, T., Rajshree, S.L., Givalois, L., Devarajan, P. V., Desrumaux, C., 2022. Intranasal Administration of nanovectorized docosahexaenoic acid (DHA) improves cognitive function in two complementary mouse models of Alzheimer's disease. Antioxidants 11, 838. https://doi.org/10.3390/antiox11050838.